The International Journal of Engineering and Science (IJES)
|| Volume || 14 || Issue 6 || June || Pages || PP 80-123 || 2025 ||
ISSN (e): 2319 – 1813 ISSN (p): 2319 – 1805

Ore Modeling and Reserve Evaluation Using Isometric Log-Ratio Transformation and Sequential Gaussian Co-Simulation – Application on The ONUPI Coal Field, Kogi State, Nigeria.

Gafar O. Oniyide[1]*, Zack A. Asitonka[1]
[1]*Federal University of Technology Akure, Akure, Nigeria.*

----------ABSTRACT----------
Mineral reserve evaluation is an extremely important stage mineral exploration and exploitation as it directly affects the economy of the mineral reserve. The Nigerian mining and quarrying sector is under performing, as a result, the benefits (such as rapid industrialization, technological innovation, raw material provision for the manufacturing industry etc.) associated with a well performing mining sector is denied the Nigerian populace. The major cause of this under performance by the sector has been attributed to lack of local and foreign investment in the mining sector, and one of the chief causes of this lack of investment is the absence of mineral reserve reports that meet international specifications, that clearly shows the profitability or non-profitability of mineral reserves in Nigeria. This researchprovides a mineral (coal) reserve report, using geological models and sequential Gaussian co-simulation of isometric log-ratio (ilr) transformed compositions, of coal proximate analysis results from the Onupi coal field. Compositional data analysis and geostatistical studies reveals significant spatial correlation among the ilr balances as indicated by the cross-semi-variograms.Geostatistical resource estimation results using simple co-kriging and co-simulation in SGeMs and Surpac computer programmes gave an estimated coal resource of 2,147,270 cm^3 in volume and a tonnage of 2,791,451 Mt. From resource classification, approximately 2,708, 250 Mt is classed as measured and indicated reserve, while 83,200 Mt is classified as inferred. Application of the simulated maps to the study area, delineates the coal boundary, and shows that high quality coals are found at the north-eastern and southern parts of the deposit, while low grade coals are concentered at the central part of the deposit.
***KEYWORDS**: Geologic Ore Modeling; Resource Estimation; Compositional Data Analysis; Geostatistics; Sequential Gaussian Simulation; Simple Kriging.*

Date of Submission: 06-06-2025 Date of acceptance: 17-06-2025

I. INTRODUCTION

Different researchers [1],[2],[3],[4],and[5] at different times, using various schemes and classifications have described the mineral coal, to satisfactorily fit their description within the scope for which it was defined. However, coal in its simplest form is a sedimentary combustible rock composed mainly of organic matter (inorganic elements present in varying quantities) formed from the burial and decomposition of plant remains by heat and pressure over a long period of time (between 25 million and 300 million years). As a source of energy, coal is extensively being used in electric power stations, and as a fuel to drive turbines and power plants for industrial purposes. [6],discussed that coal will likely remain an important input for the global cement industry for many years to come as it is essentially used to power the high temperature kiln used to mix cement raw materials into clinker. It can also be converted through various chemical processes into gaseous or liquid fuels, called synthetic fuels.

Proximate analysis is the least detailed method of coal chemical analysis when compared to other methods, but at the same time it analyzes all possible components. The four components in a proximate analysis namely, moisture (inherent water), volatile matter, ash and fixed carbon are usually reported in weight percentage. Moisture is determined by drying pulverized coal at about 38°C. As 'received moisture' is the percentage weight loss relative to the original weight. Inherent moisture is obtained by applying empirical corrections to the "as received moisture". Volatile matter (comprises primarily hydrocarbons, sulfur and carbon dioxide) refers to the additional components freed after rising the temperature to about 482°C in the absence of air. Ash is the solid residue left after complete combustion of the coal. Finally, fixed coal is not directly measured; it is the difference to 100% of the sum of the other three components[7].

Proximate analysis provides the contribution to a total of the four partial components, hence, the four parts fall in the category of compositional data [8]. In variable space, drill cores have 4 components with all of the parts having a numerical value that defines a vector mathematically. In this project our interest is in the geographical (spatial) variation of the components, each one of them is a regionalized variable, which is best modeled using geostatistics ([9], [10]). The combine use of compositional data analysis and geostatistics for coal resource evaluation have been around for decades – [11]dealt with coal reserve evaluation in Parvadah IV coal deposit, Cental Iran; [12] dealt with mapping coal ultimate analysis data of Springfield coal deposit, Indiana USA; and [13]dealt with coal quality mapping of Texas lignite. These combined methods have not been applied to Nigerian coal reserve evaluations. The most comprehensive literature on the coal resources of Nigeria by [14],indicate the methods used was non-geostatistics but the polygon method of estimation.

The aim is to apply these methods (compositional data analysis and geostatistics) to a Nigerian coal deposit, and in the future on other mineral deposits with compositional nature. Theobjectives of the study are to; (a) create a geologic model of the coal deposit within the study area; (b) model the spatial fluctuations in the coal proximate analysis components using isometric log ratio transformation in compositional data analysis and stochastic (random) stimulation in geostatistics; (c) use the results to understand and map trends and uncertainty separately for each component, and by combining the components, adequately delineate high and low quality coal within the deposit; and (d) evaluate and classify the coal reserve into measured (proven) and inferred from block models created from the geologic model.

II. MATERIALS AND METHODS

The materials used in this work are; Geovia^{TM} Surpac Software,Global Mapper,Surfer[13],Google Earth,Global Positioning System (GPS),Measuring Tape, Rule, Field Note book,Microsoft Excel Spread Sheet,Stanford Geostatistical Modeling Software (SGeMS), Compositional Data Analysis Software (CoDa Pack), andGeostatistical Software Library Computer Programme**(**GSLIB).

Geologic Ore Modeling

To create an accurate and useful geologic model of the ore, an understanding of the general geology and specific geolgy of the study area is requred, this was achieved through field investigation and data acquisition from the mining company.The geology of Nigerian coals, their origin and major subdivisions into lower and upper coal measures have been discussed by [15];[16], [17], [18],[19], and [20].Figure 1is the modified geologic map showing the location of lower and upper coal measures, the Mamu formation, and other lithologic units of the Anambra Basin in the Lower Benue Trough that hosts most of the economic coal deposits.[14]gave a detailed discussion on the general characteristics and petrology of Nigerian coals, classifying them as sub-bituminous.[21]gave a report on coal occurrences and their estimated reserves at different locations in Nigeria (Table 1). Figure 2 gives the modified map of coal occurrences in southeastern Nigeria, showing the location and their estimates.

Table 1: Coal reserves of Nigeria (from Minerals and Industry in Nigeria, GSN, 1987, after [21])

COAL			
Locality	**Geologic Unit**	**State**	**Reserves (tonnes)**
Enugu	Mamu Formation	Enugu	42,760,000
Ezimo	Mamu Formation	Enugu	29,470,000
Owukpa	Mamu Formation	Enugu	50,800,000
Inyi	Nsukka Formation	Enugu	10,160,000
Okaba	Mamu Formation	Kogi	61,200,000
Ogboyoga & Odokpono	Mamu Formation	Kogi	83,320,000
Lafia - Obi	Augu Formation	Nassarawa	32,000,000
	Total		**309,710,000**
	LIGNITE		
Obomkpa	Ogwashi-Asaba Formation	Delta	10,160,000
Ogwashi-Asaba	Ogwashi-Asaba Formation	Delta	60,960,000
	Total		**71,120,000**

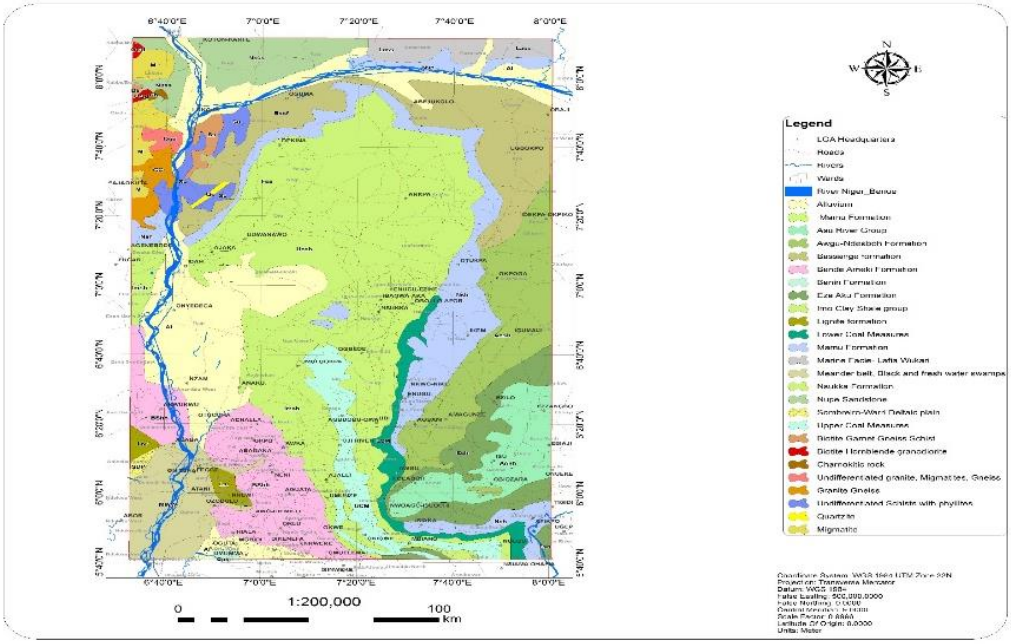

Figure 1:Geologic Map of the Mamu Formation and Upper and Lower Coal Measures in the eastern part of the Anambra Basin *(Adopted from [20])*

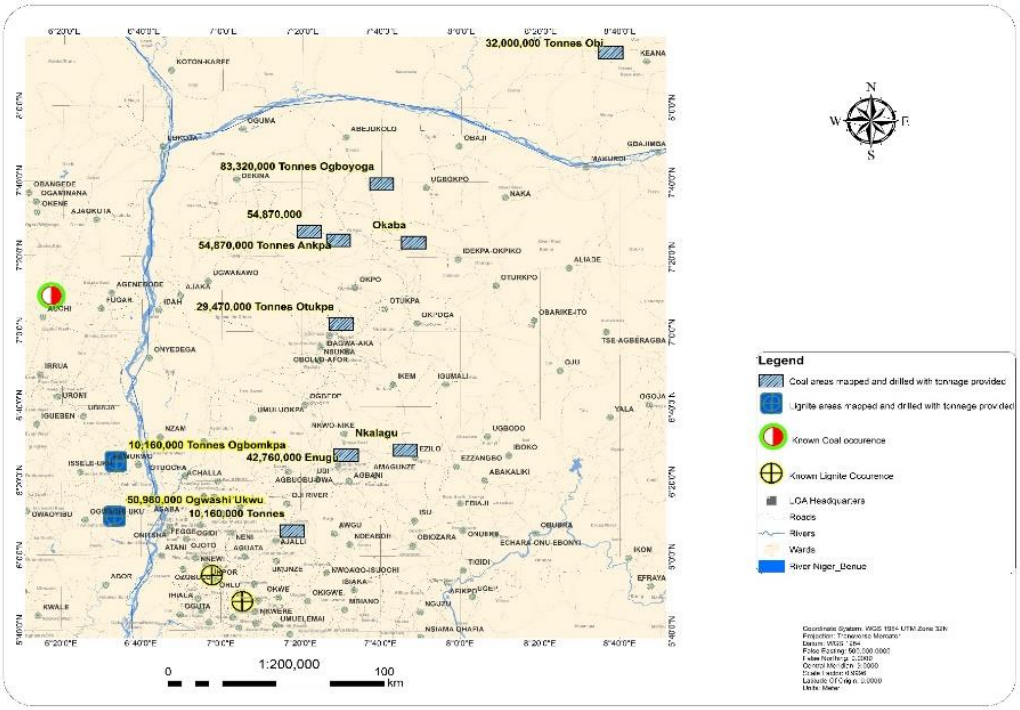

Figure 2: Map showing the location of coal occurrences in southeastern Nigeria and their estimates. Data from Minerals and Industry in Nigeria, GSN, 1987. (*Adopted from*[21])

Geology of the Study Area - Onupi (Ankpa-Okaba)

From the investigation of the Onupi coal mine, Okaba and Ankpa are very geologically similar (both are of the Mamu Formation). Field investigations which include geologic observation, and mapping of the lithological units to ascertain the stratigraphy of the mine from open cast pits and drill cores was carried out. Figure 3 and Figure 4 shows the lithology and environmental interpretationof the rock profile exposed at an open cast pit at Onupi.

In 2006, the Dangote Coal Mine Company started exploration (core drilling) and survey at Onupi, about 1.2 km south of Awo-Akpali where the company has already started coal production. At Onupi, 38 exploration holes were drilled for coring at an average drill hole spacing of 100 m. The drilling pattern is irregular (not along grid) as a result of the hilly nature of the terrain. The explored area is bounded by coordinates, Latitude: 823860 and 824777, and Longitude: 362524 and 362923 (not the exact coordinates, real coordinates are with-held because of company policy) using the Universal Transverse Mercator (UTM) coordinate system.

The area of the field investigation is approximately 367,717 m^2, and out of the 38 holes drilled 32 holes intersected coal, while five (5) holes ONPE-02, ONPE-10, ONPE-17, ONPE-20 and ONPO-03 did not intersect coal, and ONPE-22 experienced rod jam during drilling. Table 2 gives the summary of the field investigation report carried out at the study area (ONPE – Onupi Extension hole and ONPO – Onupi Old hole). Figure 5 gives the satellite map of the study area and the area bounding the drilling programme. Figure 6 shows the couture map of the study area with the drill hole locations, holes marked NC (No coal) are the holes that did not intersect coal.

The Onupi Coal Seam

The Onupi Coal Seam is normally overlain by shale, carbonaceous shale or sandy shale, but sometimes sandstone rests directly on the coal. The upper junction is normally sharp and at the base the seam grades into carbonaceous shale through a layer of shaly coal from 0.5 m to 6.49 m thick. The band of carbonaceous shale is usually thin and is underlain by sandstone or shale. Two thin coal seams are present 0.55 m and 0.51 m above the main seam in borehole ONPE-25 and ONPE-30. The undivided section of the Onupi seam is from 0.2 m to 2.5 m thick, and has an average thickness of 1.7 m.

At Onupi, from the observation of already mined (not yet reclaimed) pits, the upper coal graded into the intervening sandstone observed from pit 1 (pit 1 is about 160 m North of pit 2), while the lower coal seam could be traced into pits 2 and 3 which are about 400 m apart (Figure 5). At pit 3, the coal seam deviated North-East wards where present investigation drilling is being carried out to determine its path. This bearing if traced, is the same direction of that of the pit presently mined at Awo-Akpali.

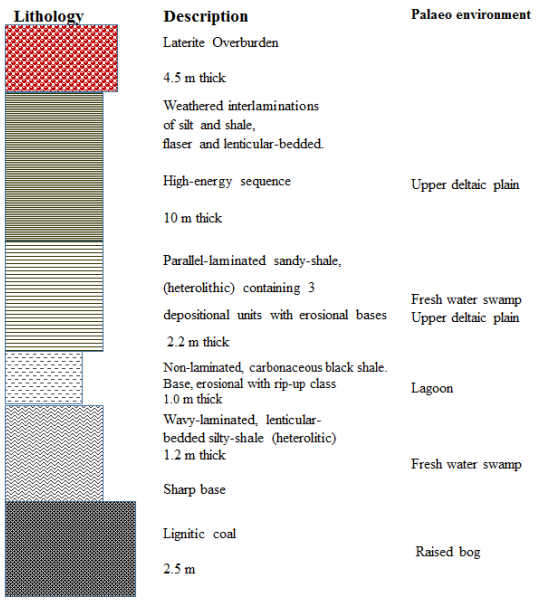

Figure 4: Lithology of the Mamu Formation (section exposed at Onupi Opencast coal mine), and environmental interpretation. (*Adopted from [20]and [21]*)

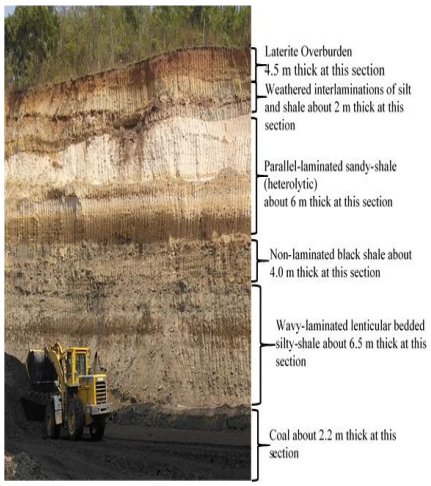

Figure 3: The stratigraphy of the sturdy area at an exposed pit.

Figure 5: Satellite Image of the study area and the area bounding the drilling programme at Onupi. Awo-Akpali is about 1 km North (using mine coordinate) of Onupi.

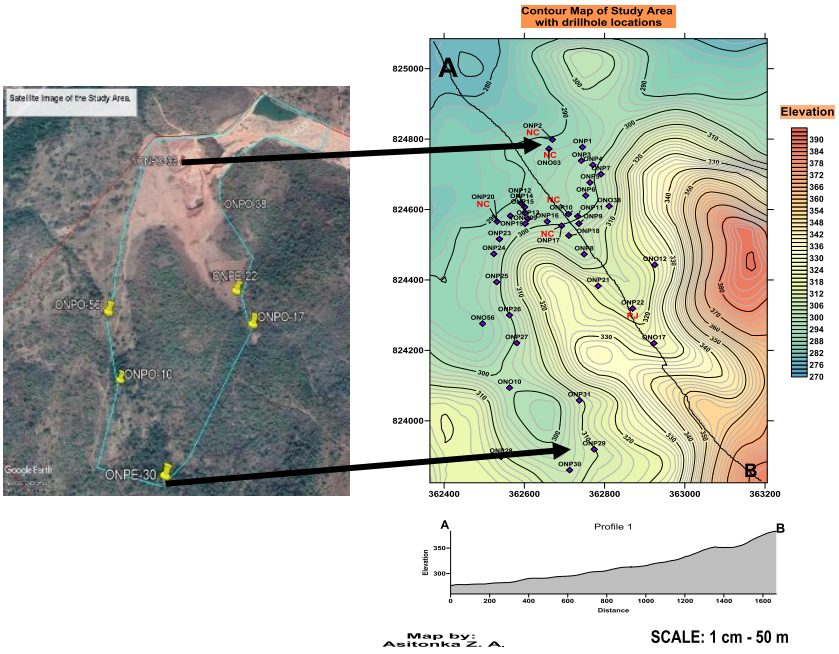

Figure 6: Couture map of the study area with the drill hole locations, holes marked NC (No coal) are the holes that did not intersect coal.

Table 2: Summary of the Field Investigation Report.

BOREHOLES DETAILS FOR ONUPI EXTENSION PITS

BH NO.	Coordinates			Coal Intersection (m)		Coal Thickness (m)	Drilled Depth (m)	Coal Roof RLs	Remarks
	Easting	Northing	Elevation (GL)	From	To				
ONPE-01	362744.98	824777.11	285.66	17. 50	18. 80	1. 30	21. 00	268.16	
ONPE-02	362670.09	824798.41	276.29	0.00	0.00	0. 00	21. 00	0.00	No Coal
ONPE-03	362742.21	824738.64	287.63	18. 50	20. 10	1. 60	24. 00	269.13	
ONPE-04	362770.96	824726.69	290.77	23. 10	24. 80	1. 00	36. 10	267.67	

ONPE-05	**362763.56**	**824676.70**	**291.75**	**23. 30**	**25. 30**	**2. 00**	**27. 00**	**268.45**	
ONPE-06	**362753.14**	**824639.71**	**292.14**	**23. 00**	**25. 5**	**2. 50**	**33. 00**	**269.14**	
ONPE-07	**362791.07**	**824700.42**	**301.05**	**34.7**	**36. 00**	**1. 30**	**39.00**	**266.35**	
ONPE-08	**362749.00**	**824473.00**	**295.81**	**29.5**	**32.05**	**2.55**	**33. 00**	**266.31**	
ONPE-09	**362736.00**	**824560.00**	**292.67**	**22.8**	**25. 10**	**2. 30**	**27. 00**	**269.87**	
ONPE-10	**362710.00**	**824587.00**	**291.05**	**0.00**	**0.00**	**0. 00**	**30. 00**	**0.00**	**No Coal**
ONPE-11	**362733.00**	**824581.00**	**291.95**	**22. 30**	**24. 00**	**1. 70**	**27. 00**	**269.65**	
ONPE-12	**362592.00**	**824618.00**	**286.65**	**21. 00**	**21. 20**	**0. 20**	**33. 00**	**265.65**	
ONPE-13	**362609.00**	**824574.00**	**289.15**	**21. 80**	**24. 00**	**2.2**	**27. 00**	**267.35**	
ONPE-14	**362601.00**	**824607.00**	**287. 40**	**21. 00**	**21. 30**	**0. 30**	**27. 00**	**266. 60**	
ONPE-15	**362602.00**	**824590.00**	**288. 10**	**21. 50**	**21. 80**	**0. 30**	**27. 00**	**267.45**	
ONPE-16	**362657.00**	**824566.00**	**290.65**	**23. 20**	**25. 40**	**2. 20**	**27. 00**	**267.45**	
ONPE-17	**362693.00**	**824554.00**	**291. 90**	**0.00**	**0.00**	**0. 00**	**27. 00**	**0.00**	**No Coal**
ONPE-18	**362711.00**	**824526.00**	**293.15**	**26. 90**	**28. 40**	**1. 50**	**30. 00**	**266.25**	
ONPE-19	**362565.00**	**824582.00**	**287.15**	**20. 70**	**21. 00**	**0. 30**	**24. 00**	**266.45**	
ONPE-20	**362532.00**	**824566.00**	**286.55**	**0.00**	**0.00**	**0. 00**	**27. 00**	**0.00**	**No Coal**
ONPE-21	**362784.00**	**824383.00**	**300.25**	**33. 80**	**35. 80**	**2. 00**	**39. 00**	**266.45**	
ONPE-22	**362870.00**	**824319.00**	**305. 30**	**0.00**	**0.00**	**0. 00**	**39. 00**	**0.00**	**Rod Jam**
ONPE-23	**362538.00**	**824516.00**	**289.25**	**21. 30**	**23. 60**	**2.3**	**30. 00**	**267.95**	
ONPE-24	**362524.00**	**824474.00**	**290.05**	**23. 60**	**25. 60**	**2. 00**	**27. 00**	**266.45**	
ONPE-25	**362531. 00**	**824394.00**	**291.15**	**24. 50**	**26.57**	**2.07**	**27. 00**	**266.65**	
ONPE-26	**362563. 00**	**824300.00**	**290.65**	**22.75**	**24.98**	**2.23**	**27. 00**	**267. 90**	
ONPE-27	**362581. 00**	**824221.00**	**289.65**	**22.64**	**24.84**	**2. 20**	**27. 00**	**267.01**	
ONPE-28	**362542. 00**	**823898.00**	**304. 20**	**38.87**	**39.42**	**0.55**	**42. 00**	**265.33**	
				40.18	**41. 60**	**1.42**			
ONPE-29	**362774. 00**	**823919.00**	**302. 90**	**41. 50**	**42. 70**	**1. 20**	**45. 00**	**261. 40**	
ONPE-30	**362713. 00**	**823860.00**	**302.25**	**38.15**	**38.56**	**0.51**	**45. 00**	**264.1**	
				39.46	**40. 90**	**1.44**			
ONPE-31	**362737. 00**	**824058.00**	**302.25**	**38.23**	**40.23**	**2. 00**	**42. 00**	**264.02**	
ONPO-03	**362661.32**	**824772.52**	**292.44**	**0. 00**	**0. 00**	**0. 00**	**28. 00**	**0. 00**	**No Coal**
ONPO-09	**362602.18**	**824559.62**	**296.25**	**22. 30**	**24. 60**	**2. 30**	**28. 00**	**273.95**	
ONPO-10	**362562.95**	**824093.90**	**300.03**	**26. 50**	**28.58**	**2.08**	**31. 00**	**273.53**	
ONPO-12	**362925.29**	**824442.99**	**312.43**	**43. 50**	**45.56**	**1.96**	**47. 50**	**273.83**	
ONPO-17	**362923.15**	**824220.32**	**315.17**	**46. 00**	**48.01**	**2.01**	**61. 00**	**269.17**	
ONPO-38	**362811.38**	**824609.48**	**305.75**	**31. 00**	**33.05**	**2.05**	**39. 00**	**274.75**	
ONPO-56	**362496. 00**	**824276.00**	**291.41**	**18. 50**	**20. 00**	**2. 30**	**23. 00**	**272.91**	

Table 3: The Survey Table

HOLE ID	DEPTH (M)	DIP (DEGREES)	ORIG_ AZIMUTH (DEGREES)
ONPE-01	21	-90	0
ONPE-02	21	-90	0
ONPE-03	24	-90	0
ONPE-04	36	-90	0
ONPE-05	27	-90	0
ONPE-06	33	-90	0
ONPE-07	39	-90	0
ONPE-08	33	-90	0
ONPE-09	27	-90	0
ONPE-10	30	-90	0
ONPE-11	27	-90	0
ONPE-12	33	-90	0
ONPE-13	27	-90	0
ONPE-14	27	-90	0
ONPE-15	27	-90	0
ONPE-16	27	-90	0
ONPE-17	27	-90	0
ONPE-18	30	-90	0
ONPE-19	24	-90	0
ONPE-20	27	-90	0
ONPE-21	39	-90	0
ONPE-22	39	-90	0
ONPE-23	30	-90	0
ONPE-24	27	-90	0
ONPE-25	27	-90	0
ONPE-26	27	-90	0
ONPE-27	27	-90	0
ONPE-28	42	-90	0
ONPE-29	45	-90	0
ONPE-30	45	-90	0
ONPE-31	42	-90	0
ONPO-03	28	-90	0
ONPO-09	28	-90	0
ONPO-10	31	-90	0
ONPO-12	47	-90	0
ONPO-17	61	-90	0
ONPO-38	39	-90	0
ONPO-56	23	-90	0

Data Acquisition and Processing

Various data which comprise drill hole survay, drill core(Figure 7) and proximate analysis, were obtained from the the mining company. The data obtatined were used to create the different data tables in microsoft excel spreadsheet for the creation of a database that was used in the various computer tools namely, Geovia Surpac (for geologic model, block model, geostatistical studies and resource estimation), Stanford Geostatistical Modeling Software (SGeMS), Compositional Data Analysis Software (CoDa Pack) – (for compositional data analysis),Surfer[13] (map creation) and GSLIB (geostatistical analysis – simulation).

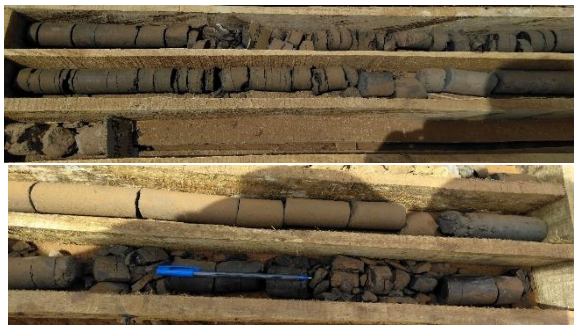

Figure 7: Images of some Drill Core Samples in core trays from Onupi Coal Mine.

The survey table (Table 3) was constructed from the downhole survey data, the geology table (surmmary is in Table 4, complete data is in Appendix B) was constructed from the drill core log analysis report (Appendix A), the collartable (Table 5) was created from the core drill and survey reports, and the assaytable (Table 6) was constructed from the coal proximate analysis report (Table 7).

Table 4: The Geology Table

HOLE ID	DEPTH_ FROM (M)	DEPTH_ TO (M)	LITHOLOGY CODE
ONPE-01	0	2	GL
ONPE-01	2	3.5	GL
ONPE-01	3.5	4	CLY
ONPE-01	4	7	CLY
ONPE-01	7	8	CLY-SDST
ONPE-01	8	11	CLY-SDST
ONPE-01	11	14	SDST
ONPE-01	14	16	SDST
ONPE-01	16	17.5	SHL
ONPE-01	17.5	18.8	C
ONPE-01	18.8	20.3	SHL
ONPE-01	20.3	21	SDST
ONPE-02	0	2	CLY-SDST
ONPE-02	2	3.5	SDST
ONPE-02	3.5	4	SHL
ONPE-02	4	7	SDST
ONPE-02	7	8	SHL
ONPE-02	8	11	SDST
ONPE-02	11	12.6	SHL
ONPE-02	12.6	14.6	SDST
ONPE-02	14.6	16	CLY-SDST
ONPE-02	16	17	SHL-SDST
ONPE-02	17	18.5	SDST
ONPE-02	18.5	20	SHL
ONPE-02	20	21	SHL
ONPE-03	0	2.4	SHL-SDST
ONPE-03	2.4	5.4	SHL-SDST
ONPE-03	5.4	8.8	SDST
ONPE-03	8.8	10.8	SDST
ONPE-03	10.8	12.4	SHL-SDST
ONPE-03	12.4	15.1	SHL
ONPE-03	15.1	16.7	SHL-SDST
ONPE-03	16.7	18.3	SHL
ONPE-03	18.3	20.1	C
ONPE-03	20.1	20.6	SHL-C
ONPE-03	20.6	22.6	SHL
ONPE-03	22.6	24	SHL-SDST
ONPE-04	0	3	SHL-SDST
ONPE-04	3	6.5	SDST
ONPE-04	6.5	9.2	SHL
ONPE-04	9.2	10.4	SDST
ONPE-04	10.4	11.2	SHL
ONPE-04	11.2	11.7	SHL-SDST
ONPE-04	11.7	12.9	SHL-SDST
ONPE-04	12.9	14.2	SHL-SDST

ONPE-04	**14.2**	**15.1**	**SHL-SDST**
ONPE-04	**15.1**	**16.2**	**SHL-SDST**
ONPE-04	**16.2**	**17.5**	**SHL-SDST**
ONPE-04	**17.5**	**18.4**	**SDST**
ONPE-04	**18.4**	**19.4**	**SHL-SDST**
ONPE-04	**19.4**	**19.9**	**SHL**
ONPE-04	**19.9**	**21.5**	**SHL**
ONPE-04	**21.5**	**22.3**	**SHL-SDST**
ONPE-04	**22.3**	**23.2**	**SHL**
ONPE-04	**23.2**	**24.8**	**C**
ONPE-04	**24.8**	**28.4**	**SHL-SDST**
ONPE-04	**28.4**	**29.9**	**SHL-C**
ONPE-04	**29.9**	**36.1**	**SHL-SDST**
ONPE-05	**0**	**2.8**	**CLY-SDST**
ONPE-05	**2.8**	**4.3**	**SHL-SDST**
ONPE-05	**4.3**	**6.3**	**SHL-SDST**
ONPE-05	**6.3**	**6.8**	**SHL**
ONPE-05	**6.8**	**9.4**	**SHL**
ONPE-05	**9.4**	**12.1**	**SDST**
ONPE-05	**12.1**	**15.1**	**SHL**
ONPE-05	**15.1**	**17.8**	**SHL-SDST**
ONPE-05	**17.8**	**19.3**	**SHL**
ONPE-05	**19.3**	**20.3**	**SDST**
ONPE-05	**20.3**	**22.3**	**SHL**
ONPE-05	**22.3**	**23.5**	**SDST**
ONPE-05	**23.5**	**25.3**	**C**
ONPE-05	**25.3**	**27**	**SHL**
ONPE-06	**0**	**3**	**CLY-SDST**
ONPE-06	**3**	**6.5**	**SHL**
ONPE-06	**6.5**	**8.5**	**SHL**
ONPE-06	**8.5**	**10**	**SHL**
ONPE-06	**10**	**12**	**SHL**
ONPE-06	**12**	**14.5**	**SDST**
ONPE-06	**14.5**	**16**	**SHL**
ONPE-06	**16**	**17.6**	**SHL-SDST**

Table 5: The Collar Table

HOLE ID	EASTING X	NORTHING Y	ELEVATION Z	MAX. DEPTH (M)	COAL_ ROOF (M)	REMARKS	HOLE_ PATH
ONPE-01	362745	824777.1	285.66	21	268.16	Coal	Straight
ONPE-02	362670.1	824798.4	276.29	21	0	No Coal	Straight
ONPE-03	362742.2	824738.6	287.63	24	269.13	Coal	Straight
ONPE-04	362771	824726.7	290.77	36.1	267.67	Coal	Straight
ONPE-05	362763.6	824676.7	291.75	27	268.45	Coal	Straight
ONPE-06	362753.1	824639.7	292.14	33	269.14	Coal	Straight
ONPE-07	362791.1	824700.4	301.05	39	266.35	Coal	Straight
ONPE-08	362749	824473	295.81	33	266.31	Coal	Straight
ONPE-09	362736	824560	292.67	27	269.87	Coal	Straight
ONPE-10	362710	824587	291.05	30	0	No Coal	Straight
ONPE-11	362733	824581	291.95	27	269.65	Coal	Straight
ONPE-12	362592	824618	286.65	33	265.65	Coal	Straight
ONPE-13	362609	824574	289.15	27	267.35	Coal	Straight
ONPE-14	362601	824607	287.4	27	266.6	Coal	Straight
ONPE-15	362602	824590	288.1	27	267.45	Coal	Straight
ONPE-16	362657	824566	290.65	27	267.45	Coal	Straight
ONPE-17	362693	824554	291.9	27	0	No Coal	Straight
ONPE-18	362711	824526	293.15	30	266.25	Coal	Straight
ONPE-19	362565	824582	287.15	24	266.45	Coal	Straight
ONPE-20	362532	824566	286.55	27	0	No Coal	Straight
ONPE-21	362784	824383	300.25	39	266.45	Coal	Straight
ONPE-22	362870	824319	305.3	39	0	Rod Jam	Straight
ONPE-23	362538	824516	289.25	30	267.95	Coal	Straight
ONPE-24	362524	824474	290.05	27	266.45	Coal	Straight
ONPE-25	362531	824394	291.15	27	266.65	Coal	Straight
ONPE-26	362563	824300	290.65	27	267.9	Coal	Straight
ONPE-27	362581	824221	289.65	27	267.01	Coal	Straight
ONPE-28	362542	823898	304.2	42	265.33	Coal	Straight
ONPE-29	362774	823919	302.9	45	261.4	Coal	Straight
ONPE-30	362713	823860	302.25	45	264.1	Coal	Straight
ONPE-31	362737	824058	302.25	42	264.02	Coal	Straight
ONPO-03	362661.3	824772.5	292.44	28	0	No Coal	Straight
ONPO-09	362602.2	824559.6	296.25	28	273.95	Coal	Straight
ONPO-10	362563	824093.9	300.03	31	273.53	Coal	Straight

ONPO-12	362925.3	824443	312.43	47.5	273.83	Coal	Straight
ONPO-17	362923.2	824220.3	315.17	61	269.17	Coal	Straight
ONPO-38	362811.4	824609.5	305.75	39	274.75	Coal	Straight
ONPO-56	362496	824276	291.41	23	272.91	Coal	Straight

Table 6: The Assay Table

HOLE ID	SAMPLE ID	DEPTH FROM (M)	DEPTH TO (M)	MOISTURE (%)	VOLATILE MATTER (%)	FIXED CARBON (%)	ASH (%)	CALORIFIC VALUE
ONPE-01	PRX-A-1	17.5	18.8	12.2	38.3	40.5	9	2478.42
ONPE-03	PRX-A-2	18.5	20.1	12.5	38.9	37.8	10.8	2411.64
ONPE-04	PRX-A-3	23.1	24.1	7.1	42.7	42.2	8	2847.6
ONPE-05	PRX-A-4	23.3	25.3	6.1	42.8	43.8	7.3	3018.96
ONPE-06	PRX-A-5	23	25.5	8.4	41.2	42	8.4	2696.4
ONPE-07	PRX-A-6	34.7	36	8.4	41.6	42	8	2797.2
ONPE-08	PRX-A-7	29.5	32.05	9	41.2	41.9	7.6	2588.04
ONPE-09	PRX-A-8	22.8	25.1	9.3	40	40.1	10.6	2454.48
ONPE-11	PRX-A-9	22.3	24	7.4	40.9	42.7	9	2865.24
ONPE-12	PRX-A-10	21	21.2	8	42.4	42.7	6.9	2940.84
ONPE-13	PRX-A-11	21.8	24	7.3	42.6	41.4	8.7	2484.72
ONPE-14	PRX-A-12	21	21.3	8	39.8	41.6	10.6	2545.2
ONPE-15	PRX-A-13	21.5	21.8	6.4	42.1	41.2	10.3	2484.72
ONPE-16	PRX-A-14	23.2	25.4	8	41.4	41.4	9.2	2492.28
ONPE-18	PRX-A-15	26.9	28.4	8.1	42.7	41.4	7.8	2520
ONPE-19	PRX-A-16	20.7	21	11.5	40.8	38.8	8.9	2613.74
ONPE-21	PRX-A-17	33.8	35.8	8.5	44	36.1	11.4	2462.54
ONPE-23	PRX-A-18	21.3	23.6	8.9	43.4	37.5	10.2	2505.38
ONPE-24	PRX-A-19	23.6	25.6	5	42.8	39.8	12.4	2638.94
ONPE-25	PRX-A-20	24.5	26.5	5.2	41.7	41.9	11.2	2790.14
ONPE-26	PRX-A-21	22.75	24.98	4.9	43.1	41.6	10.4	2790.14
ONPE-27	PRX-A-22	22.64	24.84	5.4	44.9	40.6	9.1	2732.18
ONPE-28	PRX-A-23	40.18	41.6	5.3	43.3	40.7	10.7	2757.38
ONPE-29	PRX-A-24	41.5	42.7	6.3	40.4	41.4	11.9	2777.54
ONPE-30	PRX-A-25	39.46	40.9	5.8	42.6	39.2	12.4	2623.82
ONPE-31	PRX-A-26	38.23	40.23	5.7	43.1	40.5	10.7	2656.58
ONPO-09	PRX-O-27	22.3	24.6	11.2	41.2	36.9	10.7	2487.74
ONPO-10	PRX-O-28	26.5	28.58	12.7	42.6	37.8	6.9	2512.94
ONPO-12	PRX-O-29	43.5	45.56	13.1	38.9	40.6	7.4	2734.7
ONPO-17	PRX-O-30	46	48	12.8	39.7	38.6	8.9	2613.49
ONPO-38	PRX-O-31	31	33.05	10.5	39.6	33.5	16.4	2311.34
ONPO-56	PRX-O-32	18.5	20	12	40.7	38	9.3	2563.34

Table 7: Proximate Analysis Report of Selected Coal samples from Onupi

PROXIMATE ANALYSIS OF COAL SAMPLES FROM ONUPI

HOLE ID	Sample ID	Coal Seam Thickness	Depth of bottom Seam	Proximate Analysis				Calorific Value	
		m	m	Moisture (%)	Volatile (%)	Fixed Carbon (%)	Ash (%)	C.V (BTU/Lb.)	C.V (Kcal/kg)
ONPE-01	PRX-A-1	1. 30	21. 00	12.20	38.30	40.50	9.00	9835.00	2478.42
ONPE-03	PRX-A-2	1. 60	21. 00	12.50	38.90	37.80	10.80	9570.00	2411.64
ONPE-04	PRX-A-3	1. 00	24. 00	7.10	42.70	42.20	8.00	11300.00	2847.60
ONPE-05	PRX-A-4	2. 00	36. 10	6.10	42.80	43.80	7.30	11980.00	3018.96
ONPE-06	PRX-A-5	2. 50	27. 00	8.40	41.20	42.00	8.40	10700.00	2696.40
ONPE-07	PRX-A-6	1. 30	33. 00	8.40	41.60	42.00	8.00	11100.00	2797.20
ONPE-08	PRX-A-7	2.55	39.00	9.00	41.20	41.90	7.60	10270.00	2588.04
ONPE-09	PRX-A-8	2. 30	33. 00	9.30	40.00	40.10	10.60	9740.00	2454.48
ONPE-11	PRX-A-9	1. 70	27. 00	7.40	40.90	42.70	9.00	11370.00	2865.24
ONPE-12	PRX-A-10	0. 20	30. 00	8.00	42.40	42.70	6.90	11670.00	2940.84
ONPE-13	PRX-A-11	2.2	27. 00	7.30	42.60	41.40	8.70	9860.00	2484.72
ONPE-14	PRX-A-12	0. 30	33. 00	8.00	39.80	41.60	10.60	10100.00	2545.20
ONPE-15	PRX-A-13	0. 30	27. 00	6.40	42.10	41.20	10.30	9860.00	2484.72
ONPE-16	PRX-A-14	2. 20	27. 00	8.00	41.40	41.40	9.20	9890.00	2492.28
ONPE-18	PRX-A-15	1. 50	27. 00	8.10	42.70	41.40	7.80	10000.00	2520.00
ONPE-19	PRX-A-16	0. 30	24. 00	11.50	40.80	38.80	8.90	10372.00	2613.74
ONPE-21	PRX-A-17	2. 00	39. 00	8.50	44.00	36.10	11.40	9772.00	2462.54
ONPE-23	PRX-A-18	2.3	30. 00	8.90	43.40	37.50	10.20	9942.00	2505.38
ONPE-24	PRX-A-19	2. 00	27. 00	5.00	42.80	39.80	12.40	10472.00	2638.94
ONPE-25	PRX-A-20	2.07	27. 00	5.20	41.70	41.90	11.20	11072.00	2790.14
ONPE-26	PRX-A-21	2.23	27. 00	4.90	43.10	41.60	10.40	11072.00	2790.14
ONPE-27	PRX-A-22	2. 20	27. 00	5.40	44.90	40.60	9.10	10842.00	2732.18
ONPE-28	PRX-A-23	1.42	42. 00	5.30	43.30	40.70	10.70	10942.00	2757.38
ONPE-29	PRX-A-24	1. 20	45. 00	6.30	40.40	41.40	11.90	11022.00	2777.54
ONPE-30	PRX-A-25	1.44	45. 00	5.80	42.60	39.20	12.40	10412.00	2623.82
ONPE-31	PRX-A-26	2. 00	42. 00	5.70	43.10	40.50	10.70	10542.00	2656.58
ONPO-09	PRX-A-27	2. 30	28. 00	11.20	41.20	36.90	10.70	9872.00	2487.74
ONPO-10	PRX-A-28	2.08	31. 00	12.70	42.60	37.80	6.90	9972.00	2512.94
ONPO-12	PRX-A-29	1.96	47. 50	13.10	38.90	40.60	7.40	10852.00	2734.70
ONPO-17	PRX-A-30	2.01	61. 00	12.80	39.70	38.60	8.90	10371.00	2613.49
ONPO-38	PRX-A-31	2.05	39. 00	10.50	39.60	33.50	16.40	9172.00	2311.34
ONPO-56	PRX-A-32	2. 30	23. 00	12.00	40.70	38.00	9.30	10172.00	2563.34

Coal Seam Modeling in Geovia Surpac

A three-dimensional (3D) model of the coal seam was created using the portions of the drill holes that intersected the coal. Drill hole sections with coal thickness less than 0.5 m were not included in the model, as they were considered too thin and not economic to extract. Figure 8 shows the 3D model of the Onupi coal seam in a grid, and Figure 9 shows the 3D model of the coal seam in the section view with the drill holes indicating the depth at which the coal seam was intersected. Table 8 gives the major lithological units in the study area and their respective codes used for geologic modeling of the coal deposit.

Table 8: Major Lithological Units in the study area and modeled Codes

LITHOLOGY	MODELED CODE
LATERITE, GRAVEL	GL
CLAY	CLY
CLAY-SANDSTONE	CLY-SDST
SANDSTONE	SDST
SHALE	SHL
COAL	C
SHALY-SANDSTONE	SHL-SDST

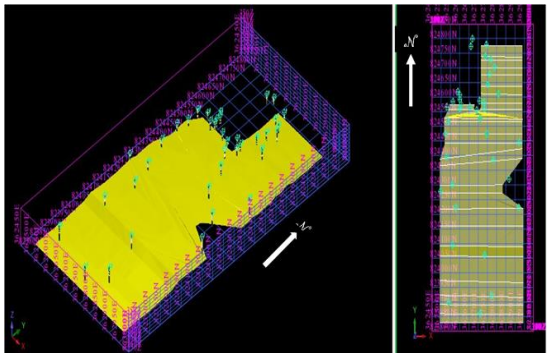

Figure 8: Lift -3D solid model of the coal seam in a 50 x 50 x 10 m grid. Right shows the model in the XY-plane.

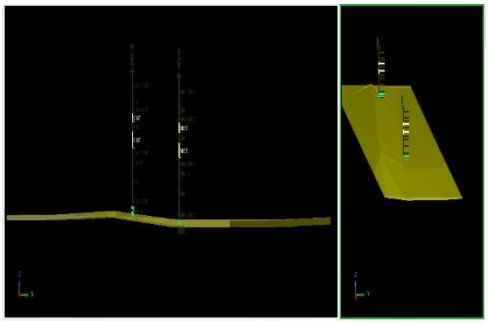

Figure 9: shows the 3D model of the coal seam in the section view with the drill holes showing the different rock units.

Exploratory Data Analysis (EDA)

The first step in any geostatistical analytical exercise is exploratory data analysis (EDA). This step is necessary to detect any potential problems, such as errors in the dataset, and lack of stationarity. When using sequential gaussian simulation, we must make the decision of stationarity for the data, for us to be able to carry out any statistical analysis[22]. Server lack of stationarity is worthy of special attention. Zones with different statistics (bimodal distributions) are processed separately, outliers if detected should be well investigated and dealt with using appropriate methods (either by top-cutting them or converting them to the minimum values if found at the tail or maximum values if found at the head of the distribution). EDA also

provides the variable distributions and basic summary statistics. Figure 10 shows the histograms of the proximate analysis results for the coal components and some basic summary statistics.

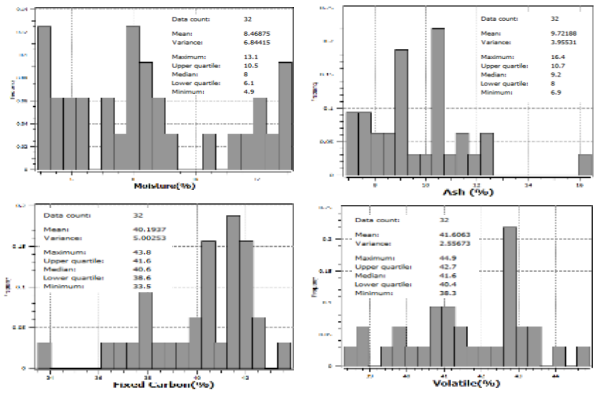

Figure 10: Histograms of the proximate analysis results for the coal components and some basic summary statistics.

Compositional Data Analysis (CoDa)

Coal proximate analysis is a form of compositional data or compositions which consist of observations that are part of a whole (sum up to a constant) and carry relative information [23]. It is proven that straight application of standard statistical and geostatistical methods to compositional data will always expose the results to inconsistencies and non-optimality [24], [25],and[26].

[27], stated that the main problem of geostatistical analysis of regionalized compositions in their raw form can be stated in terms of covariances which are subjected to nonstochastic controls. Therefore, to get a better understanding of the proximate analysis and the relationship between the variables namely, Ash (A), Fixed carbon (FC), Volatile Matter (VM) and Moisture Content (M), the compositional data analytical approach, more precisely the Isometric Log-ratio (ilr) transformation method introduced by [28], which involved the transformation of the raw (constrained or closed) data into unconstrained ilr-coordinates known as balances by defining a sequential binary partition (SBP) for the 4-part (Ash, Fixed carbon, Volatile Matter and Moisture content) compositions.

The procedure for ilr transformation of compositional date and the mathematical details involved are summarized in the proceeding sections, details can be found in [28]. The comparison of the compositional and non-compositional approaches, and the problems associated with neglecting the compositional nature of proximate analysis data in resource estimation are not discussed in this work but are well presented by[13], [12] and [11].

The compositional Data Package (CoDa Pack) [29]was used for defining the SBP and carrying out the ilr data transformation. The full closed system with D parts (in our case D = 4) is transformed into D – 1 balance coordinates, and the relationship of these balances with the parts is through log-ratios of geometric means of parts. The SBP is defined based on the mutual relationship of the parts that is Ash, Fixed carbon, Volatile matter, and Moisture. Considering the Onupi coal compositional data set with D parts, a SBP matrix will have D columns and D – 1 rows (4 columns and 3 rows), each row indicates a group of parts, Equation 1. The participation of a part in a group is coded by +1, -1 and 0; whereby convention, +1 indicates the part in the numerator, -1 the parts in the denominator, and 0 the parts not participating in the partition. The compositional bi-plot (Figure 11) that is based on the centered log-ratio (clr) transformation is one of the most popular ways to jointly represent the variables due to its connection to principal component analysis (PCA) [30]. The bi-plot is a 2-D representation of the singular value decomposition (SVD), where the individual data points are represented as dots and the variables are represented as rays. The length of a ray is proportional to the standard deviation of the variable it represents. If two rays are near each other, the variables might be highly associated. If three or more vertices of rays are aligned, a compositional linear interaction between the parts may exist and should be investigated. The links between the vertices of rays, are proportional to the standard deviation of the simple log-ratio of the variables corresponding to the rays[31]. The cosine of the angle between the two links closely approximates the correlation coefficient between the corresponding simple log-ratios [26]. If this angle is orthogonal (90 degrees), the two simple log-ratios are possibly uncorrelated [12].

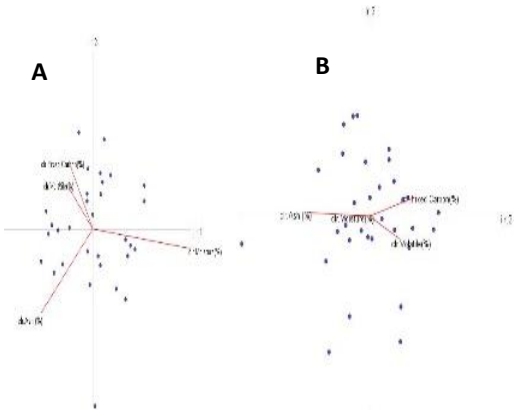

Figure 11: clr biplot of proximate analysis data of the coal samples: (A) 1st (ilr_1) and 2nd (ilr_2) PCs (98% explained variance), (B) 2nd (ilr_2) and 3rd (ilr_3) PCs.

From the centered log-ratio (clr) biplots (Figure 11) the behavior of parts (Ash, Fixed carbon (FC), Volatile matter (VM), and Moisture (M)) can be virtualized. The SBP matrix (Equation 1) was constructed with +1, -1 and 0 values, using the interpretation of the relationship among the parts as depicted in the biplots. The ilr transformation leads to three (3) balances denoted by ilr_1, ilr_2, and ilr_3. The principal components shown by the clr biplot of proximate analysis data of the Onupi coal represents 98% of the cumulative variance (Figure 11andTable 9). Based on the inverse relationship of moisture (M) with the other parts (Ash, FC, VM) (Figure 11(A)), and considering the fact that the clr (moisture (%)) has the longest ray, it was decided to mark moisture (%) with -1 at the first row of the SBP matrix. This procedure was repeated for Ash (%) based on the clr biplot of Figure 11(B). The full SBP matrix for the parts is defined by Equation 1.

$$SBP = \begin{array}{c} \\ ilr_1 \\ ilr_2 \\ ilr_3 \end{array} \begin{array}{c} \begin{array}{cccc} M & Ash & FC & VM \end{array} \\ \begin{bmatrix} -1 & +1 & +1 & +1 \\ 0 & -1 & +1 & +1 \\ 0 & 0 & -1 & +1 \end{bmatrix} \end{array} \begin{array}{c} r_i s_i \\ 31 \\ 21 \\ 11 \end{array} \quad (1)$$

Table 9: Principal Components PCs of the clr transformed values

	PC1	PC2	PC3
CLR.M (%)	0.85	-0.17	0.01
CLR.VM (%)	-0.21	0.36	-0.76
CLR.FC(%)	-0.19	0.55	0.64
CLR.ASH (%)	-0.45	-0.74	0.11
CUMULATIVE PROPORTION EXPLAINED	0.76	0.99	1

Isometric Log-ratio Transformation (ilr)

Based on SBP matrix, the ilr balances are given by Equation 2.

$$ilr_i = \sqrt{\frac{ri \; x \; si}{ri + si}} \; In \left[\frac{g(z+)}{g(z-)}\right] \quad , i = 1, 2, \ldots D - 1 \quad (2)$$

where r_i is the number of +1 values in *i*-th row of SBP, s_i is the number of -1 values in the same row, g (z_+) and g (z_-) are the geometric means of parts which corresponding values in the SBP are +1 and -1, respectively. Equations 3, 4 and 5 gives the expressions used to calculate the ilr balances.

For example, the balances ilr_1,ilr_2, and ilr_3 for the proximate analysis are calculated below

$$ilr_1 = \sqrt{\frac{3 \times 1}{3+1}}\, ln\left[\frac{(FC \times VM \times Ash)^{1/3}}{(M)}\right] \quad (3)$$

$$ilr_2 = \sqrt{\frac{2 \times 1}{2+1}}\, ln\left[\frac{(FC \times VM)^{1/2}}{(Ash)}\right] \quad (4)$$

$$= \sqrt{\frac{2}{3}}\, ln\left[\frac{(FC \times VM)^{1/2}}{(Ash)}\right]$$

$$ilr_3 = \sqrt{\frac{1 \times 1}{1+1}}\, ln\left[\frac{(VM)}{(FC)}\right] \quad (5)$$

$$= \sqrt{\frac{1}{2}}\, ln\left[\frac{(VM)}{(FC)}\right]$$

$$ilr_1 = \sqrt{\frac{3}{4}}\, ln\left[\frac{(40.5 \times 38.3 \times 9.0)^{1/3}}{(12.2)}\right] = 0.5888 \quad (6)$$

$$ilr_2 = \sqrt{\frac{2}{3}}\, ln\left[\frac{(40.5 \times 38.3)^{1/2}}{(9.0)}\right] = 1.2053 \quad (7)$$

$$ilr_3 = \sqrt{\frac{1}{2}}\, ln\left[\frac{(38.3)}{(40.5)}\right] = -0.0395 \quad (8)$$

Considering a drill hole (ONPE-01, PRX-A-1 from our data set in Table 7) with proximate analysis [12.2 9.0 40.5 38.3] for [M Ash FC VM] respectively. There Isometric Log-ratio (ilr) balances are computed as follows,

Back Transformations (ilr Inverse Function)

Geostatistical estimation and simulation are best performed on distributions that follow an approximately normal distribution, as such the ilr transformed data were used for estimation and simulation for resources evaluation because they follow a symmetric distribution. In order to cross-validate the simulated values and evaluate the uncertainty, it is necessary to back-transform the simulated ilr's to the original data space using the ilr inverse function (Equation 8).

By defining clr transformation (Equation 9) and ilr transformation in matrix form (Equation 9), the ilr inverse function is given by Equation 11, [23].

$$clr\ (\mathbf{Z}\ (x_i)) = ln\ \frac{xi}{g(Z(xi)}\ ,\ i = 1, 2, \ldots, N \quad (9)$$

$$ilr\ (\mathbf{Z}\ (x_i)) = \phi.\ clr\ (\mathbf{Z}\ (x_i)),\ i = 1, 2, \ldots, N \quad (10)$$

$$\mathbf{Z}\ (x_i) = \boldsymbol{C}.\ exp\ (\phi^{T}.\ ilr\ (\mathbf{Z}\ (x_i))),\ i = 1, 2, \ldots, N \quad (11)$$

where **N** is the sample size, clr **(Z(x_i))** is the set of transformed compositions by clr transformation, g**(Z(x_i))** is the sample geometric mean of the composition, ilr **(Z(x_i))** is the vector of transformed balances, ϕ is the (D, D-1) constant matrix, which is
defined by (Equation 9), $Z(x_i)$ is the compositions at location $\mathbf{x}_i$ and $\boldsymbol{C}$ is the closure constant - one over the sum of elements in the vector $\boldsymbol{\phi^{T}.\ ilr.}$

where v_{ij} denotes the element of i-th row and j-th column in the SBP matrix. r_i and s_i were explained in Equatio the back transformation of the ilr balances gotten in Equation 3 tc ilr inverse function.

$$\phi_{i,j} = \begin{cases} 0 & \text{if } v_{ij} = 0, \\ \sqrt{\frac{si}{ri\,.(si+ri)}} & \text{if } v_{ij} = +1, \\ -\sqrt{\frac{ri}{si\,.(si+ri)}} & \text{if } v_{ij} = -1, \end{cases} \quad (12)$$

Firstly, the constant matrix (ϕ) is defined using Equation 12, its transpose (ϕ^T) is later defined, followed by the matrix multiplication (ϕ^T x ilr_i*) of the transposed constant matrix and the ilr values earlier evaluated, and taking their exponents (designated here as $\mathbf{p}_i$) which satisfies the first part of Equation 8. The closure constant $\mathbf{C}$, which is a ratio of the constant sum (100% in our case) over the sum of the elements in the vector $\mathbf{p}_i$ is then computed. The product of the closure constant $\mathbf{C}$ and corresponding $\mathbf{p}_i$ according to the ordering of the parts in the SBP matrix gives the back transformed raw values ($Z_{(i)}$*), which satisfies the other part of Equation 8. The above steps are detailed below.

$$\phi = \begin{pmatrix} -\sqrt{\frac{3}{1x(1+3)}} & \sqrt{\frac{1}{1x(1+3)}} & \sqrt{\frac{1}{1x(1+3)}} & \sqrt{\frac{1}{1x(1} \\ 0 & -\sqrt{\frac{2}{1x(1+2)}} & \sqrt{\frac{1}{2x(1+2)}} & \sqrt{\frac{1}{2x(1+2)}} \\ 0 & 0 & -\sqrt{\frac{1}{1x(1+2)}} & \sqrt{\frac{1}{1x(1+2)}} \end{pmatrix}$$

$$\phi^T \text{ x } ilr^* = \begin{pmatrix} (-\sqrt{\frac{3}{4}}\,.\,ilr_1) \\ (\sqrt{\frac{1}{12}}\,.\,ilr_1) - (\sqrt{\frac{2}{3}}.\,ilr_2) \\ (\sqrt{\frac{1}{12}}.\,Ilr_1) + (\sqrt{\frac{1}{6}}\,.\,ilr_2) - (\sqrt{\frac{1}{2}}.\,ilr_3) \\ (\sqrt{\frac{1}{12}}.\,ilr_1) + (\sqrt{\frac{1}{6}}\,.\,ilr_2) + (\sqrt{\frac{1}{2}}\,.\,ilr_3) \end{pmatrix}$$

$$\phi = \begin{pmatrix} -\sqrt{\frac{3}{4}}\sqrt{\frac{1}{12}}\sqrt{\frac{1}{12}}\sqrt{\frac{1}{12}} \\ 0\ -\sqrt{\frac{2}{3}}\sqrt{\frac{1}{6}}\sqrt{\frac{1}{6}} \\ \ulcorner\ \ulcorner \end{pmatrix}$$

In which case **p** (exponent of the matrix product) is evaluated thus,

$$\mathbf{p} = \phi^T \text{ x } ilr_i = \begin{pmatrix} exp(-\sqrt{\frac{3}{4}}\,.\,ilr_1) \\ exp(\sqrt{\frac{1}{12}}\,.\,ilr_1 - \sqrt{\frac{2}{3}}.\,ilr_2) \\ exp(\sqrt{\frac{1}{12}}.\,Ilr_1 + \sqrt{\frac{1}{6}}\,.\,ilr_2 - \sqrt{\frac{1}{2}}.\,ilr_3) \\ exp(\sqrt{\frac{1}{12}}.\,ilr_1 + \sqrt{\frac{1}{6}}\,.\,ilr_2 + \sqrt{\frac{1}{2}}\,.\,ilr_3) \end{pmatrix}$$

$$\phi^T = \begin{pmatrix} -\sqrt{\frac{3}{4}}00 \\ \sqrt{\frac{1}{12}} - \sqrt{\frac{2}{3}}\ 0 \\ \sqrt{\frac{1}{12}}\sqrt{\frac{1}{6}} - \sqrt{\frac{1}{2}} \\ \ulcorner\ \ulcorner\ \ulcorner \end{pmatrix}$$

Consequently,

$$\mathbf{p_1} = xp(-\sqrt{\tfrac{3}{4}}\,.\,ilr_1)$$

$$\mathbf{p_2} = exp(\sqrt{\tfrac{1}{12}}\,.\,ilr_1 - \sqrt{\tfrac{2}{3}}.\,ilr_2)$$

$$\mathbf{p_3} = exp(\sqrt{\tfrac{1}{12}}.\,Ilr_1 + \sqrt{\tfrac{1}{6}}\,.\,ilr_2 - \sqrt{\tfrac{1}{2}}.\,ilr_3)$$

$$\mathbf{p_4} = exp(\sqrt{\tfrac{1}{12}}.\,ilr_1 + \sqrt{\tfrac{1}{6}}\,.\,ilr_2 + \sqrt{\tfrac{1}{2}}\,.\,ilr_3)$$

Applying the above expressions on the earlier computed ilr for drill hole ONPE-01 we have,

$$\mathbf{p_1} = \exp(-\sqrt{\frac{3}{4}} * 0.5888 = 0.600545$$

$$\mathbf{p_2} = \exp(\sqrt{\frac{1}{12}} * 0.5888 - \sqrt{\frac{2}{3}} * 1.2053) = 0.443025$$

$$\mathbf{p_3} = \exp(\sqrt{\frac{1}{12}} * 0.5888 + \sqrt{\frac{1}{6}} * 1.2053 - \sqrt{\frac{1}{2}} * - 0.0395) = 1.993614$$

$$\mathbf{p_4} = \exp(\sqrt{\frac{1}{12}} * 0.5888 + \sqrt{\frac{1}{6}} * 1.2053 + \sqrt{\frac{1}{2}} * 0.0395) = 1.885319$$

The closure term becomes,

$$\mathbf{C} = \frac{100}{p1+p2+p3+p4} = \frac{100}{0.600545+0.443025+1.993614+1.885319} = 20.31487,$$

and the back transformed values ($Z_{(i)}$*) for sample ONPE-01 are given below.

Z_1*	M*	c x p1	20.31487 * 0.600545	12.2
Z_2*	Ash*	c x p2	20.31487 *0.443025	9
Z_3*	FC*	c x p3	20.31487 *1.993614	40.5
Z_4*	VM*	c x p4	20.31487 *1.885319	38.3

Figure 12shows the histograms of the isometric log-ratio (ilr) transformed values (balances: ilr_1, ilr_2, and ilr_3) and some basic summary statistics. Comparing the variances (standard deviations) of the raw data and the ilr transformed values (Table 10andTable11), the raw values show higher variance in the distribution. The histograms of the raw data (Figure 10) also show a skewed distribution for the variables Ash and FC. The ilr histograms in Figure 12 gives a more symmetrical distribution of the variables. More so, performing preliminary statistical tests on the ilr transformed values revealed no censored and outlier data. Table 12 gives the raw data values and their corresponding clr, ilr transformed, and biplot generated (UD) values generated using the CoDa pack software.

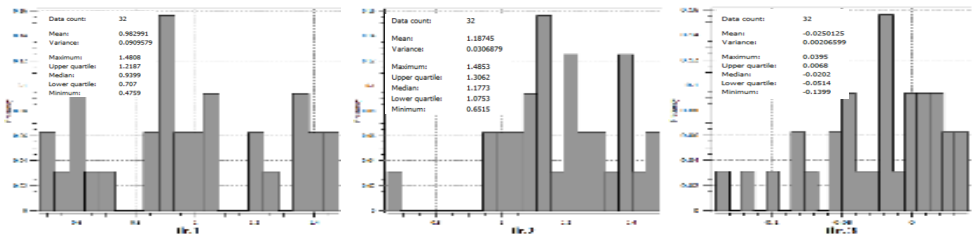

Figure 12: Histograms of the isometric log-ratio (ilr) balances: ilr_1, ilr_2, and ilr_3.

Table 10: Summary Statistics of the Raw Proximate Analysis Data

CLASSICAL STATISTICS SUMMARY: RAW DATA							
NA'S: 0							
SAMPLE SIZE: 32							
STATISTICS							
	Mean	**Std.Dev**	**0**	**25**	**50**	**75**	**100**
MOISTURE (%)	8.4688	2.5749	4.9	6.3	8.1	11.2	13.1
VOLATILE (%)	41.6062	1.5738	38.3	40.7	41.7	42.8	44.9
FIXED CARBON (%)	40.1937	2.2014	33.5	38.8	40.7	41.9	43.8
ASH (%)	9.7219	1.9575	6.9	8.4	9.3	10.7	16.4

Table 11: Summary Statistics of the ilr Transformed Data

CLASSICAL STATISTICS SUMMARY: FOR THE ILR TRANSFORMED DATA							
NA'S: 0							
SAMPLE SIZE: 32							
STATISTICS							
	Mean	**Std.Dev**	**0**	**25**	**50**	**75**	**100**
ILR.1	0.983	0.2969	0.4759	0.8343	0.9768	1.2635	1.4808
ILR.2	1.1875	0.1724	0.6515	1.0853	1.2053	1.35	1.4853
ILR.3	-0.025	0.0447	-0.1399	-0.0485	-0.0199	0.0119	0.0395

Table 12: Raw date values and their corresponding clr, ilr transformed, and biplot generated (UD) values

SAMPLE	MOISTURE (%)	ASH (%)	FIXED CARBON (%)	VOLATILE (%)	RES ID.	C.V (KCAL/KG)	CLR. MOISTURE (%)	CLR. VOLATILE (%)	CLR.FIXED CARBON (%)	CLR. ASH (%)	ILR.1	ILR.2	ILR.3	UD1	UD2	UD3
PRX-A-1	12.2	9	40.5	38.3	0	2478.42	-0.50992	0.634097	0.689949	-0.81413	0.5888	1.2053	-0.0395	0.390544	-0.05268	0.067611
PRX-A-3	12.5	10.8	37.8	38.9	0	2411.64	-0.52392	0.61135	0.582665	-0.67001	0.6050	1.0346	0.0203	0.339923	-0.22315	0.030925
PRX-A-4	7.1	8	42.2	42.7	0	2847.6	-0.92394	0.87016	0.858381	-0.80046	1.0669	1.3626	0.0083	-0.04701	0.189003	-0.00815
PRX-A-5	6.1	7.3	43.8	42.8	0	3018.96	-1.02479	0.923454	0.94655	-0.84521	1.1833	1.4535	-0.0163	-0.14267	0.30378	0.002357
PRX-A-6	8.4	8.4	42	41.2	0	2696.4	-0.79991	0.790295	0.809527	-0.79991	0.9237	1.3062	-0.0136	0.082315	0.108651	0.023315
PRX-A-7	8.4	8	42	41.6	0	2797.2	-0.79013	0.809739	0.819309	-0.83892	0.9124	1.3500	-0.0068	0.102045	0.147983	0.010872
PRX-A-8	9	7.6	41.9	41.2	0.3	2588.04	-0.72255	0.798664	0.815512	-0.89163	0.8343	1.3870	-0.0119	0.185943	0.16899	0.012235
PRX-A-9	9.3	10.6	40.1	40	0	2454.48	-0.76277	0.696098	0.698595	-0.63193	0.8808	1.0853	-0.0018	0.08009	-0.11592	0.041752
PRX-A-11	7.4	9	42.7	40.9	0	2865.24	-0.91453	0.795122	0.838191	-0.71878	1.0560	1.2537	-0.0305	-0.05766	0.086275	0.045003
PRX-A-12	8	6.9	42.7	42.4	0	2940.84	-0.79864	0.869071	0.876121	-0.94656	0.9222	1.4853	-0.0050	0.119417	0.281042	-0.00911
PRX-A-13	7.3	8.7	41.4	42.6	0	2484.72	-0.91871	0.845271	0.816698	-0.74326	1.0608	1.2854	0.0202	-0.05665	0.111209	-0.0095
PRX-A-14	8	10.6	41.6	39.8	0	2545.2	-0.88362	0.720801	0.765035	-0.60221	1.0203	1.0983	-0.0313	-0.05371	-0.07157	0.067121
PRX-A-15	6.4	10.3	41.2	42.1	0	2484.72	-1.05543	0.828316	0.806706	-0.57959	1.2187	1.1407	0.0153	-0.24016	0.002952	0.012267
PRX-A-16	8	9.2	41.4	41.4	0	2492.28	-0.85686	0.786979	0.786979	-0.71771	0.9894	1.2281	0.0000	0.002115	0.044059	0.019269
PRX-A-18	8.1	7.8	41.4	42.7	0	2520	-0.814	0.848332	0.817414	-0.85174	0.9399	1.3755	0.0219	0.079782	0.174354	-0.02132
PRX-A-19	11.5	8.9	38.8	40.8	0	2613.74	-0.55653	0.709807	0.659545	-0.81282	0.6426	1.2227	0.0355	0.340412	-0.03508	-0.0099
PRX-A-20	8.5	11.4	36.1	44	0	2462.54	-0.84597	0.798149	0.600252	-0.55243	0.9768	1.0219	0.1399	-0.02837	-0.17728	-0.09167
PRX-A-21	8.9	10.2	37.5	43.4	0	2505.38	-0.78976	0.79465	0.648531	-0.65342	0.9119	1.1227	0.1033	0.055779	-0.08753	-0.06785
PRX-A-22	5	12.4	39.8	42.8	0	2638.94	-1.28245	0.864653	0.791982	-0.37419	1.4808	0.9818	0.0514	-0.52915	-0.10384	-0.00632
PRX-A-23	5.2	11.2	41.9	41.7	0	2790.14	-1.23393	0.847911	0.852696	-0.46668	1.4248	1.0753	-0.0034	-0.45495	-0.01694	0.036327
PRX-A-24	4.9	10.4	41.6	43.1	0	2790.14	-1.26643	0.907857	0.872434	-0.51386	1.4623	1.1464	0.0250	-0.47787	-0.05570	-0.00191
PRX-A-25	5.4	9.1	40.6	44.9	0	2732.18	-1.16432	0.953718	0.853048	-0.64245	1.3444	1.2622	0.0712	-0.33976	-0.13842	-0.06128
PRX-A-26	5.3	10.7	40.7	43.3	0	2757.38	-1.21038	0.89007	0.828145	-0.50784	1.3976	1.1161	0.0438	-0.42071	-0.01091	-0.01545
PRX-A-27	6.3	11.9	41.4	40.4	0	2777.54	-1.09425	0.76403	0.788481	-0.45826	1.2635	1.0080	-0.0173	-0.31021	-0.11261	0.061581
PRX-A-28	5.8	12.4	39.2	42.6	0	2623.82	-1.16616	0.827833	0.744655	-0.40632	1.3466	0.9737	0.0588	-0.39993	-0.13949	-0.01054
PRX-A-29	5.7	10.7	40.5	43.1	0	2656.58	-1.15342	0.869639	0.807418	-0.52364	1.3319	1.1122	0.0440	-0.35705	-0.00601	-0.01412
PRX-A-30	11.2	10.7	36.9	41.2	0	2487.74	-0.61229	0.690236	0.58001	-0.65796	0.7070	1.0558	0.0779	0.243502	-0.18993	-0.03061
PRX-A-31	12.7	6.9	37.8	42.6	0	2512.94	-0.42272	0.787533	0.667987	-1.03128	0.4881	1.4375	0.0845	0.534115	0.136045	-0.08475
PRX-A-32	13.1	7.4	40.6	38.9	0	2734.7	-0.4121	0.676281	0.719054	-0.98323	0.4759	1.3725	-0.0302	0.534483	0.085835	0.037857

PRX-A-33	12.8	8.9	38.6	39.7	0	2613.49	-0.46808	0.6638 26	0.635727	-0.83 147	0.5 405	1.2 094	0.01 99	0.438 013	-0.066 23	0.008 975
PRX-A-34	10.5	16. 4	33.5	39.6	0	2311.34	-0.73338	0.5940 71	0.426788	-0.28 748	0.8 468	0.6 515	0.11 83	0.025 293	-0.559 92	-0.018 74
PRX-A-35	12	9.3	38	40.7	0	2563.34	-0.52978	0.6915 44	0.622902	-0.78 467	0.6 117	1.1 773	0.04 85	0.361 459	-0.087 05	-0.016 24

Mapping the attributes in the original variable space

Figure 13 and Figure 14 shows the maps of the proximate analysis on a 15 x 15 m grid, giving a not too comprehensive insights about the spatial fluctuations of the attributes – Moisture, Ash, Fixed Carbon and Volatile Matter. These maps were generated using the Geostatistical Software Library (Gslib) [32] for windows (WinGslib) software.

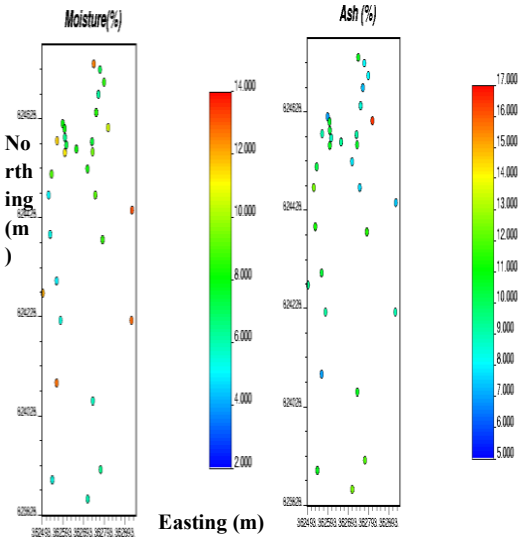

Figure 13: Post map of proximate analysis components, Moisture-M (%) and Ash -A (%)

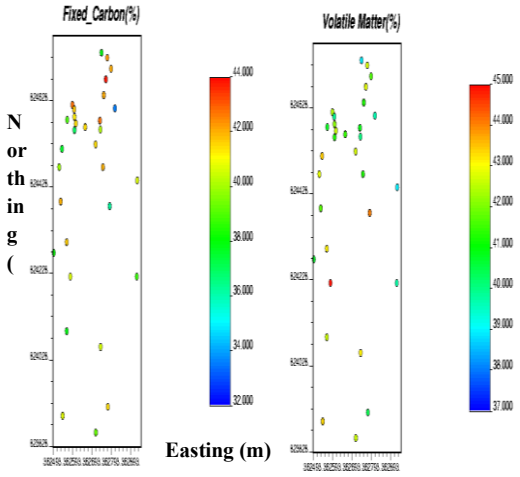

Figure 14: Post map of proximate analysis components, Fixed Carbon-FC (%) and Volatile Matter- VM (%)

Normality Test of the balances

Sequential Gaussian Simulation (SGS) is the method chosen to generate realizations (probable estimates) in this study (see sections 2.7.2 and 2.7.3 for details). SGS requires that the frequency distribution (histogram) of all variables must follow standard normal distributions (distributions with zero means and unit variance often designated as N[0,1]).

To test for the normality of our balances, the Kolmogorov-Smirnov statistics D_{KS}, was used. The results of D_{KS}stats are in Table 13. If the D_{KS}value is less than 0.1, it is acceptable to assume normality for the balance [33].

Table 13: Kolmogorov-Smirnov Statistics Results

BALANCES	DISTANCE (D_{KS})	P-VALUE
ILR.1	0.0950	0.9084
ILR.2	0.0799	0.9764
ILR.3	0.1247	0.6561

From the D_{KS} results, normality can be assumed for the balances ilr.1 and ilr.2 and not for ilr.3. As a result, normality was not assumed for the three balances, and the balances were transformed to the normal distribution (normal score -Nscore) before SGS was performed.

Geostatistics

Variogram Model Fitting and Interpretation (Variography)

The first step in most application of two-point geostatistics requires modeling of semi-variograms (measure of dissimilarity of a variable over distance) and cross-semivariograms (measure of dissimilarity of two or more correlated variables over distance). Detail discussions on the concepts of variogram calculation, variogram modeling and interpretation (variography) would not be done here. Here, we would define some important concepts and present a general procedure in variogram modeling and interpretation as it pertains to this work. For detail and in-depth understanding see, [32],[34], and [9].

$$\gamma(h) = \frac{1}{2N(h)} \sum_{a=1}^{N(h)} (Z(u_a) - Z(u_a + h))^2 \qquad (13)$$

Variogram – this is a measure of dissimilarity over distance. Calculated as $\frac{1}{2}$ (one-half) of the average squared difference of values separated by a lag distance (vector (h)), Equation 13 below gives the semi-variogram expression,

Where,
$\gamma(h)$ is the variogram,
N is the number of pairs at a given lag distance (h)
(h), is the lag distance (vector),
$Z(u_a)$ is the tail value of the variable at location u_a,
$Z(u_a + h)$ is the head value of the variable at location $(u_a + h)$

The precise term is semi-variogram (its' called variogram if we remove the $\frac{1}{2}$ (one-half)), but in practice the term variogram is used. The $\frac{1}{2}$ is used so that the covariance function and variogram may be related directly. Equation 14 gives the covariance function which is a measure of similarity among variables over a lag vector h.

$$C_x(h) = \sigma_x^2 - \gamma_x(h) \qquad (14)$$

Where;
$C_x(h)$ is the covariance of the attribute that are separated by a lag distance h,
σ_x^2 is the variance of the attribute, usually called the sill,
$\gamma_x(h)$ is the variogram at the lag distance (h).

Cross-semivariogram – is the measure of cross variability (dissimilarity) of two different attributes. It is defined as $\frac{1}{2}$ of the average product of the spatial difference of two or more different attributes separated by lag vector (distance (h)). Equation 15 is the cross-semivariogram function given in terms of two variables z and y.

$$\gamma_{ZY}(h) = \frac{1}{2N(h)} \sum_{a=1}^{N(h)} (Z_a - Z'_a)(Y_a - Y'_a) \qquad (15)$$

Where;
$\gamma_{ZY}(h)$ is the cross-semivarigram of two different attribute.
Z_a is the value of attribute Z at the tail of pair a andZ'_a is
the correspondinghead value.
The locations of the two values Z_a and Z'_a are separated
by the vector h with specified directions and distance tolerance.
$(Y_a - Y'_a)$ is the corresponding spatial difference of the other attribute Y.

More so, Figure 15 gives a summary of experimental variogram interpretation and variogram model parameter extraction from a fitted model. The main objective of fitting a model to the variogram is to define the geostatistical parameters namely, Range(s), Sill and Nugget.

Range (a) - This is the distance at which the variogram structure reaches the sill. Its measure is read from the lag distance axis.

Sill (C + Co) - This is the population variance, variance of the distribution under study. At the sill correlation is zero, below the sill correlation is positive and above the sill correlation is negative.

Nugget (Co) - This is the point variance – the variance between any two points/samples in the distribution. A low nugget indicates a low variance between points and a high nugget indicates high variability between points in the distribution. The nugget effect can be determined using the nugget ratio relation in Equation 16.

$$Nugget\ ratio = \frac{Nugget}{sill}\ x\ 100 = \frac{Co}{C + Co}\ x\ 100 \qquad (16)$$

Low – nugget ratio	< 25%	
Medium – nugget ratio		25-50%
High – nugget ratio	50-75%	
Extreme – nugget ratio		>75% [35].

The following general guidelines can be used in variogram model fitting;

i. Variograms with less number of pairs can be ignored
ii. Nugget (Co) can be obtained from the crossed tangential line of some first variogram points to the gamma $\gamma(h)$ axis.
iii. The sill (Co + C) is approximately equal or close to the population variance. – Tangential line will cross the sill line at distances $\frac{2}{3}a$ (two-third of range), so that the range (a) can be defined.
iv. Variogram model fitting must consider the experimental variogram near the origin, and then regard the variogram with high number of pairs.
v. Interpretation of nugget variance for variogram with angle tolerance > 90° (omnidirectional) is helpful in anticipating the magnitude of nugget variance.

Nugget (point variance): **0.002 (bright red dotted lines)** Note the behavior at the origin to definethe type of structure, **spherical (linear)**, **exponent**, or **gaussian. In this case, linear**

Variogram Interpretation and Model fitting

Sill (variance): **0.013 (green line)**

Look for the directions of continuities (major, semi-major and minor) to define the ranges.
Major direction of continuity: **60°** azm;
with range **32**
Semi-major direction is orthogonal (90°) to the major direction.In this case **150°** with range **16**
Minor direction of continuity: **Vertical** with range**6**

Directions of continuity and ranges are used to define the search neighborhood for estimation or

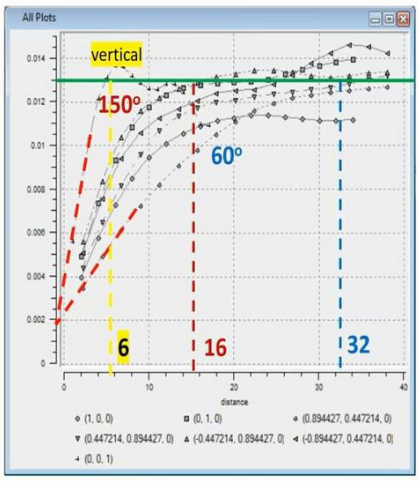

Figure 15: Variogram interpretation and modeling. Modified after[9]

2.7.2 Conditional Simulation

The details on conditional simulation and its various types such as sequential gaussian simulation, direct simulation, indicator simulation, etc, its advantages over kriging and its applications for different problems are well documented in various literatures ([32], [36], and [37]) and geostatistical journals. Therefore, detail discussion on conditional simulation and its mathematical relations will not be discussed here. The focus here will be on sequential gaussian co-simulation (SGCS) (which in practice is not very different from sequential gaussian simulation SGS) with full-cokriging.

The choice for SGCS was made for this work because of its practicality, its efficiency in honouring the data – spatial fluctuations, the histogram, the variogram and also due to its ability to enable uncertainty (error) analysis through many equiprobable realizations that maybe required to represent a stabilized variance for the attribute of interest.

On account of the practical similarity between Sequential Gaussian simulation (SGS) and SGCS, a brief description of the concept and procedureof SGS is given, this is to aid in understanding the slight difference between both methods.

SGS is a Gaussian-based method of conditional simulation [38], [10]. This method uses data transformed to a Gaussian distribution 'Nscore' with a zero mean and a unit variance N[0,1] (Gaussian anamorphosis), which is then used to simulate spatial distribution of the variable of interest.

Simulated realization is achieved by defining a random path through the grid nodes including the conditioning data, which has been migrated to the nearest grid nodes and considered as hard data. A sequential neighbourhood of the target node is established, which includes hard data (original data) and already simulated nodes (soft data). The combination of the hard and soft data is used to calculate a local conditioning distribution and derive a simulated value at the target node. The simulated value is determined using Equation 17,

$$Z^*_{SGS} = Z^*_{SK} + \delta_K(U) \quad (17)$$

Where,
Z^*_{SGS} is the SGS simulated value
Z^*_{SK} simple kriging estimate
δ_K standard deviation of the kriging estimate
(U) is a random normal function

Furthermore, conditional simulation generates quantitative models of the attribute of interest, reproducing the data histogram and their spatial variability. However, because the conditional simulation techniques are based on the Monte Carlo stochastic (random) algorithm, it generates unlimited number of equiprobable models (realizations) of the attribute of interest. All realizations honour statistical and geostatistical characteristics of the constraining data, however, they differ in details. The higher the variability of the data and less samples available for constraining the models the larger degree of the differences between realizations. Thus, by statistical analysis of the differences between simulated realizations the uncertainty of the geostatistical model can be accurately quantified[39].

Sequential Gaussian Cosimulation (SGCS) with Full-Cokriging Option

SGCS an extension of SGS, is proposed as a means for simulating models of several continues variables. It reproduces the distribution and the auto- and cross-variograms of the variables together with their values where they are known [40]. Detailed discussion on the algorithm, and the formulations of the procedure and concepts of SGCS with full cokriging can be found in [40].

With respect to the ilr balances, Table 14 shows how they were grouped based on their correlation and measure of variance into primary and secondary variables for the simple cokriging and cosimulation algorithm.

Table 14: Grouping of the ilr balances for simulation

SIMULATE	PRIMARY VARIABLE (Z)	SECONDARY VARIABLE (Y)
ILR.1	ilr.1	ilr.2
ILR.2	ilr.2	ilr.3
ILR.3	ilr.3	ilr.2

To simulate ilr.1, ilr.1 was taken as the primary variable and ilr.2 as the secondary variable. To simulate for ilr.2, ilr.2 is taken as the primary variable and ilr.3 as the secondary variable, and to simulate ilr.3, ilr.2 was used as the secondary variable.

The following gives details of the simple kriging (SK) and cokriging algorithm and give reasons why SK was chosen as the linear regression estimator. As earlier stated, SGS requires that the random variable be stationary, it is proper that simple kriging which requires a stationary mean be used as the linear regression estimator for our balances, since they are in 'gaussian/normal space' N[0,1] with a stationary mean of zero (m = 0). Equation 18 gives the SK estimator for one variable in its stationary form.

$$Z_{SK}^{*}(u) = \sum_{a=1}^{n} \lambda_{a(u)} Z_{(ua)} + \left[1 - \sum_{a=1}^{n} \lambda_{a(u)}\right] m \qquad (18)$$

Equation 16 gives the simple cokriging estimator for two variable Z and Y, primary and secondary.

$$Z_{COK}^{*}(u) = \sum_{a=1}^{n1} \lambda_{a1}(u) Z(u_{a1}) + \sum_{a=2}^{n2} \lambda_{a2}(u) Y'(u'_{a2}) + \left[1 - \left(\sum_{a=1}^{n1} \lambda_{a1}(u) + \sum_{a=2}^{n2} \lambda_{a2}(u)\right)\right] m \qquad (19)$$

Since we are working in 'gaussian space' with a zero mean (m = 0), the terms in the square brackets in Equation 15 equates to zero, and the SK cokriging estimator reduces to Equation 20,

$$Z_{COK}^{*}(u) = \sum_{a=1}^{n1} \lambda_{a1}(u) Z(u_{a1}) + \sum_{a=2}^{n2} \lambda_{a2}(u) Y'(u'_{a2}) \qquad (20)$$

Where,
λ_{a1} are the weights applied to the $n1$ Z samples, (samples of the primary variable within the search neighborhood).
λ'_{a2} are the weights applied to the $n2$ Y samples, (samples of the secondary variables within the search neighborhood).
$Z_{COK}^{*}(u)$ is the cokriged estimate that forms part of the ccdf on which Monte Carlo simulation will be applied to draw out realizations,
$Z(u_{a1})$ is the primary variable at the location u_{a1}
$Y'(u'_{a2})$ is the secondary variable at location u'_{a2}

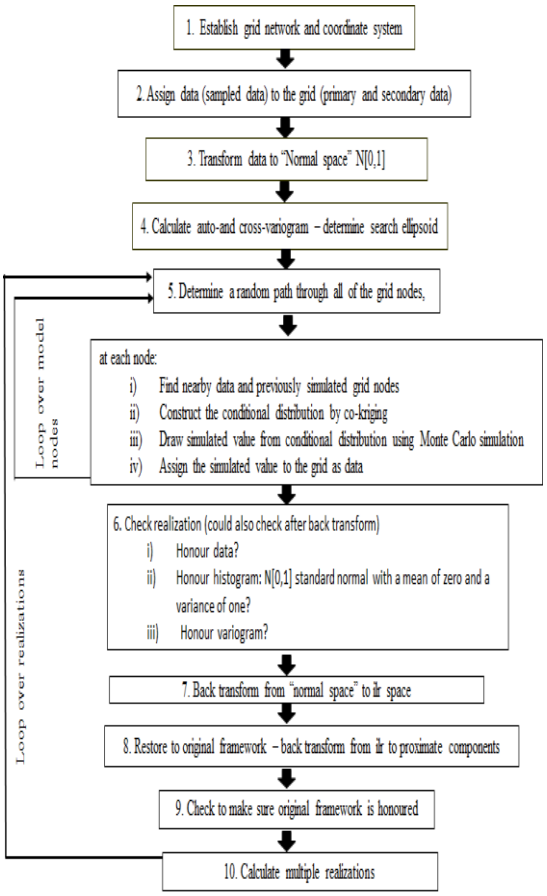

Figure 16: Steps in Sequential Gaussian Cosimulation (SGCS) used in this work.

Figure 16 shows the work flow of the steps involved in sequential gaussian cosimulation undertaken in this work, in the same vain Figure 17,Figure 18 andFigure 19 gives an illustration of the transformation of the ilr balances from 'ilr space' to 'gaussian space' with their normal score omnidirectional variograms and the variogram model parameters given in Table 15.

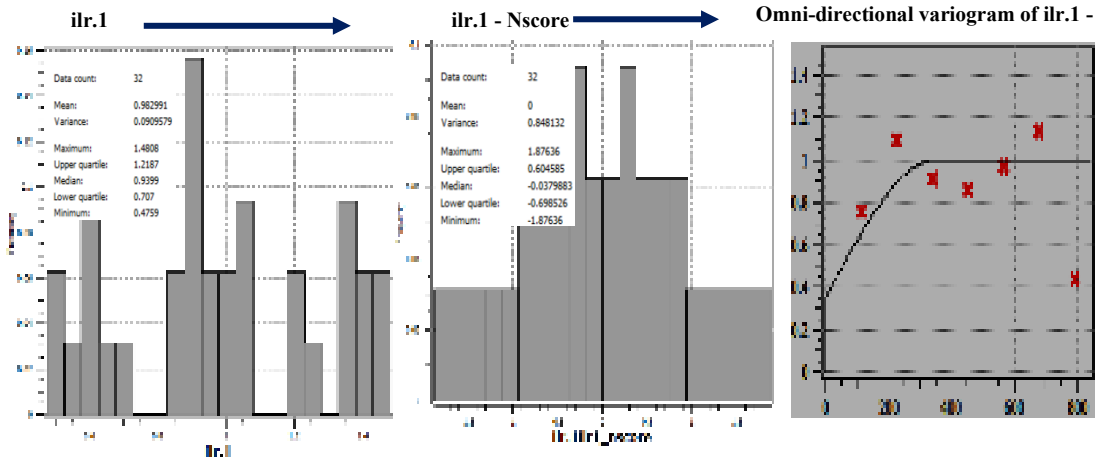

Figure 17: Transformation of ilr.1 to normal space N[0,1] and its omni-directional

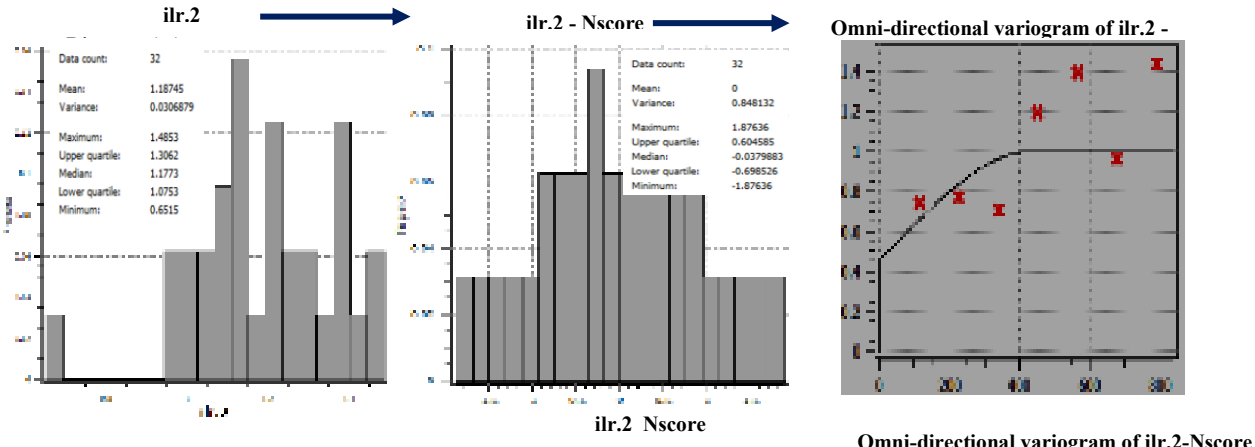

Figure 18: Transformation of ilr.2 to normal space N[0,1] and its omni-directional variogram

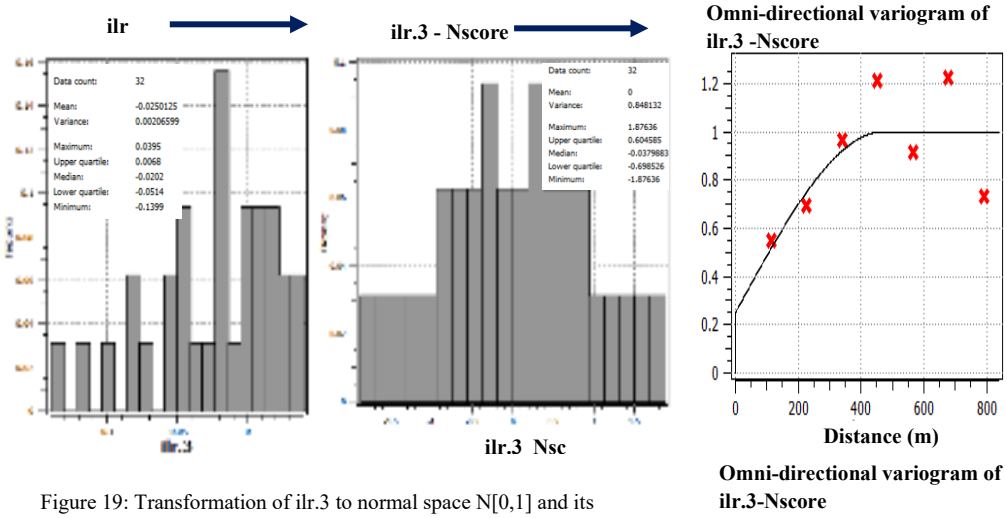

Figure 19: Transformation of ilr.3 to normal space N[0,1] and its

RESULTS AND DISCUSSION

Modeling the Anisotropy (Semi-variograms and Cross-variograms)

Using the nugget ratio relation (Equation 16) to determine the nugget effect of the ilr balance, values ranging from 33-50% (medium – nugget ratio) were obtained this indicates the variance between points in the distribution can be tolerated for modeling purposes.

More so, Figure 20 shows the auto- and cross-semivariograms and the fitted variogram models for the ilr balances. Although anisotropy was observed in the variogram, it was not significant, consequently isotropic variogram models were fitted. Table 15 and Table 16 gives the results of the variogram models and parameters for the ilr balances and the raw proximate components respectively. The variogram models were fitted using the Stanford Geostatistical Modeling Software (SGeMS) an open-source computer package.

A notable feature from the spatial continuity analysis plots in Figure 20 is the significant spatial correlation between the balances depicted by the cross-semivariogram (ilr.1 vs ilr.2, ilr.1 vs ilr.3, and ilr.2 vs ilr.3). As a result of this spatial interaction, cokriging and cosimulation methods were chosen for simulation (estimation), details are in the next section.

Table 15: Variogram Model Parameters for each of the ilr balances

ILR BALANCES	MODEL	NUGGET (CO)	SILL-NUGGET (SILL CONTRIBUTION)	MIN. RANGE (A) (M)	MAX. RANGE(A) (M)
ILR.1	spherical	0.03	0.06	350	450
ILR.2	spherical	0.015	0.015	350	450
ILR.3	spherical	0.001	0.001	350	450
	Normal Transformed (Nscore) ilr balance (Sill = 1)				
ILR.1	spherical	0.25	0.75	350	450
ILR.2	spherical	0.45	0.55	350	450
ILR.3	spherical	0.25	0.75	350	450

Table 16: Variogram Model Parameters for each of the proximate analysis components

COMPONENT	MODEL	NUGGET	SILL- NUGGET (SILL CONTRIBUTION)	MIN. RANGE (A) (M)	RANGE(A) (M)
MOISTURE	spherical	4.30	2.54	350	450
ASH	spherical	2.50	1.45	350	450
FIXED CARBON	spherical	2.30	2.70	350	450
VOLATILE MATTER	spherical	0.6	2.56	350	450

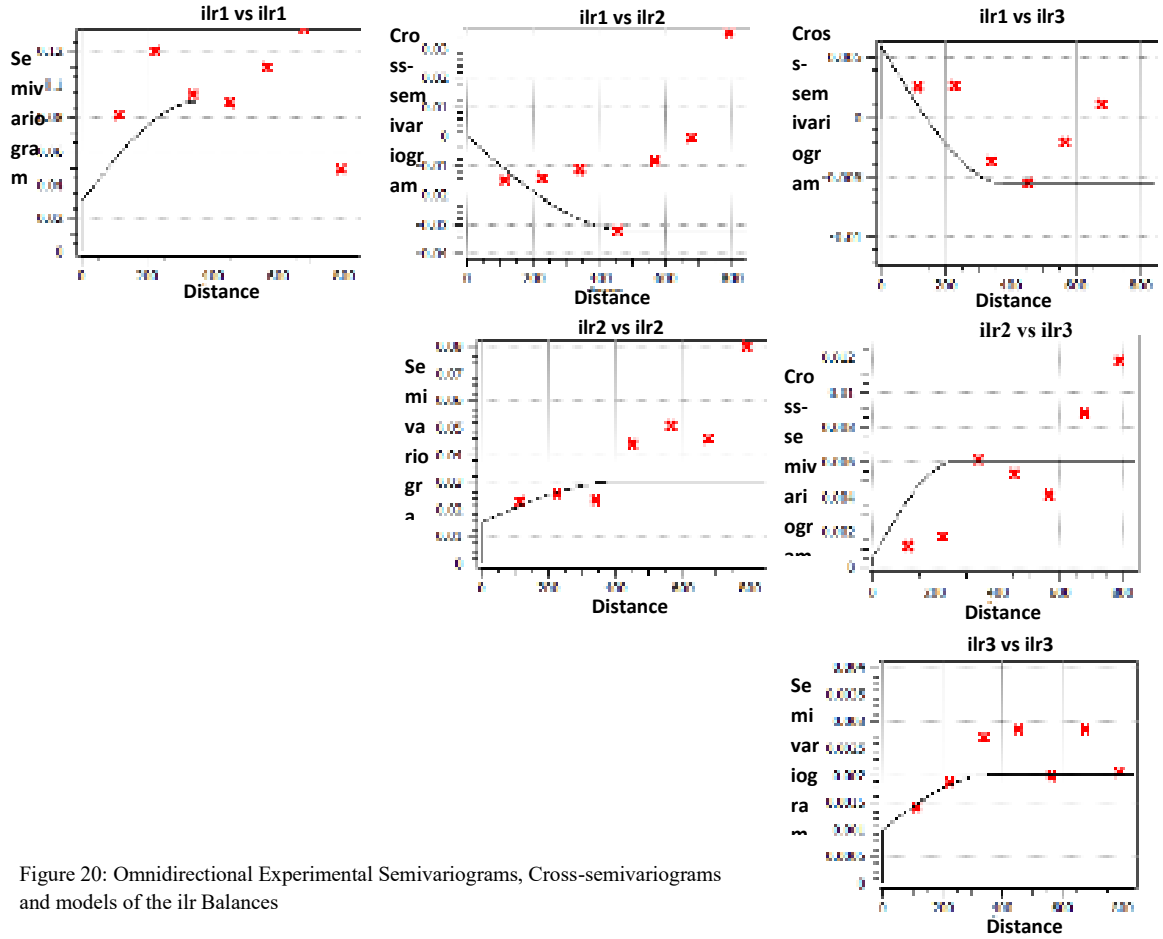

Figure 20: Omnidirectional Experimental Semivariograms, Cross-semivariograms and models of the ilr Balances

Co-simulation with Simple Cokriging

Owing to the spatial correlation between the ilr balances (Figure 20), cosimulation with simple cokriging was used to draw realizations (estimates). The SGeMS software was used for the cosimulation (cosgsim) on a 15 x 15 m grid, which gave 28350 nodes (cells). 100 realizations were drawn for each ilr balance to give us a reasonable statistic from which to make inference. In all 8,505,000 realizations were drawn for the three ilr balances (28350 x 100 = 2,835,000 for each. 2,835,000 x 3 = 8, 505,000).

Figure 21 shows the SGCS maps for realization #99 for all balances. Realization #99 was not chosen randomly; it has the best spatial fluctuations that corresponds to the original ilr balances and also reflects the inverse relation of ash and moisture to the other components.

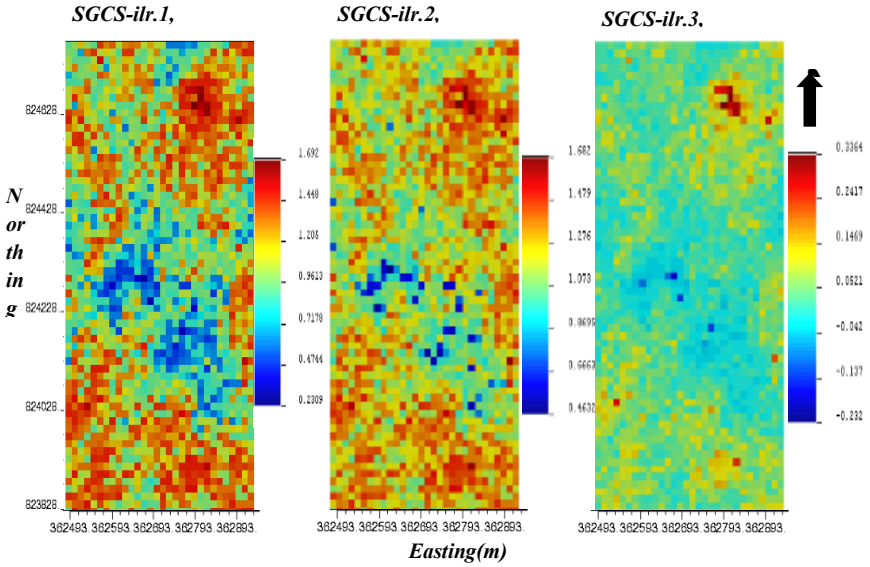

Figure 21: Sequential Gaussian Cosimulation Maps for the three-isometric

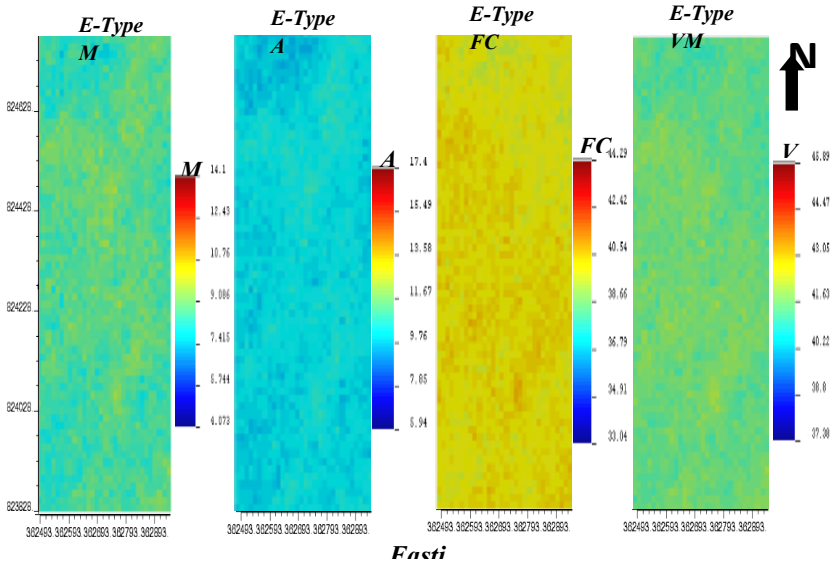

Figure 22: Sequential Gaussian Cosimulation E-Type Maps for the four-part proximate analysis components on a 15 x 15 m grid

Simulation Post-Processing – Computing the E-Type Map

For compositional data, the averaging (calculation of the arithmetic mean) has to be done among the realizations of the transformed values, such as Figure 21, and then back-transform all average maps, in our case, those for ilr.1, ilr.2 and ilr.3.

Mean-value maps, also called E-type maps, convey the same idea of kriging, only that the expected value, instead of being derived analytically (using the kriging algorithm), is calculated numerically (the sum of all node values divided by the total number of realizations). Hence, this single map per attribute, although unique and minimizing the mean square error, has the disadvantage of smoothing, which is obvious when comparing them to any realization, such as those in Figure 23. Figure 22 shows the E-type map for the four-part proximate analysis (M, Ash, FC and V). At any cell in the E-type maps, the sum of the values adds to 100% if the realizations are derived from ilr maps.

transformation

The final step is the back transformation, which is done with the three simulated balances ($ilr^*(u_i)$) exactly as illustrated in section 2.6.2 using the ilr inverse function. The simulated values of each of the ilr balances were extracted, and thereafter imported into CoDa Pack were the ilr-raw transformation option was used to back-transform the values. The paring of realizations must be done at random, because the three sets of 100 realizations were each generated at random, pairing the realizations in the same sequence as they were generated is an acceptable and convenient alternative. For example, the first cell for realization #99 of ilr.1 is paired with the first cell for realizations #99 for ilr.2 and ilr.3, and so on. The back-transformation results in 4 numbers, one for each proximate analysis part. The process is completed upon transforming the last cell for the last triplet of realizations. Figure 23shows the results upon back transforming the balances for the last cell for all 3 realizations #99.

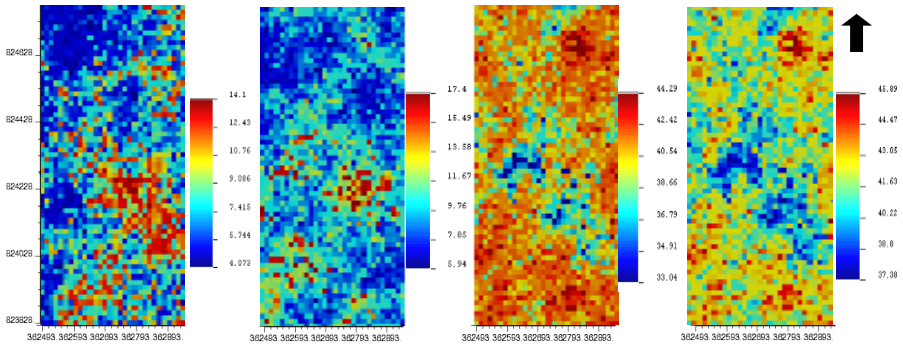

It can be observed from Figure 23 that the better coals (with FC values ranging from 40 – 44%) are found in the North-eastern and southern parts of the deposit, while the low-grade coals are mostly concentrated in the central part of the deposit. The inverse relationship between ash and fixed carbon is clearly depicted by the maps. Additionally, the similar spatial fluctuations of volatile matter and fixed carbon is clearly demonstrated. This implies that in areas where there are high-grade coals, high volatile matter contents should be expected.

Furthermore, the E-type (mean) maps of the 4-part components (Figure 22)are not very informative because they are too smooth (have similar patterns like the kriged maps – this is one of the disadvantages of kriging and why simulation is preferred to kriging). Although the E-type maps give insights as regards to the general trends of the components.

Model Validation

A very important aspect in geostatistical modeling, is the validation of the models, this is done to verify if the estimated or simulated values honours the original data, honours the original histogram, and the spatial continuity plots (variogram).

To carry out the validation of our geostatistical model, we plotted quantile-quantile/percentile-percentile (QQ/PP) plots, Histograms and variograms between raw (original) and simulated (model) values. Figures 24, 25, 26, 27 and Figure 28 shows these validation plots.

The QQ/PP plots are used to compare the similarities between two distributions. If the distributions plot exactly on the 45° line, they are classed as the same, and there is no significant difference in their moments. From Figure24 and Figure 25, it can be observed that our model did not do badly, as both distributions came close to the 45° line. Although there are some deviations, especially at the tails, but things look very similar at the middles of both distributions. The measure of these deviations can be ascertained by comparing the means and variances of both distributions given at the top left corner of the plots.

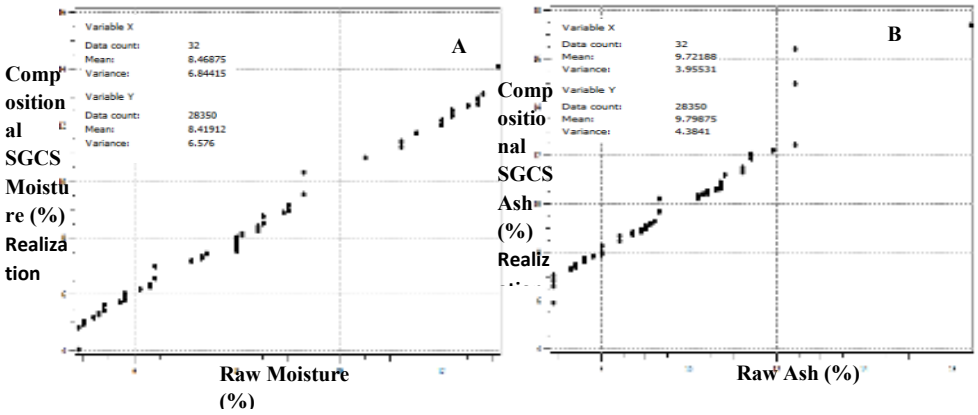

Figure 24: A. QQ/PP plot of Raw Moisture Vs SGCS Moisture. B. QQ/PP plot of Raw Ash vs SGCS Ash.

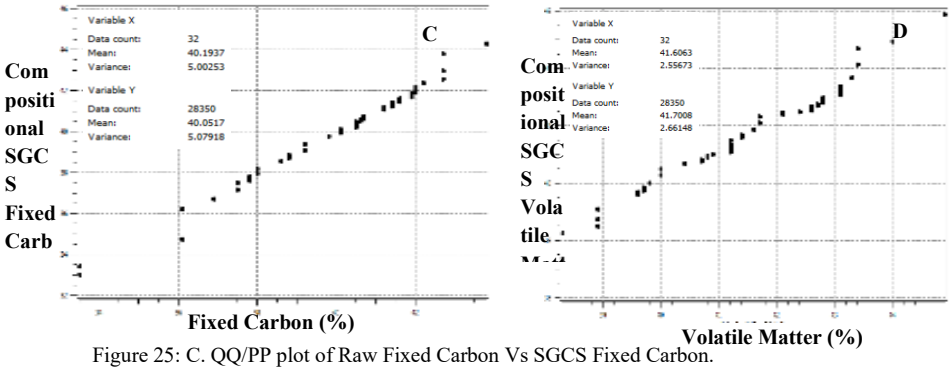

Figure 25: C. QQ/PP plot of Raw Fixed Carbon Vs SGCS Fixed Carbon.
D. QQ/PP plot of Raw Volatile Matter vs SGCS Volatile Matter.

Figure26 and Figure 27 gives the histogram of the distribution (raw and simulated). The histogram also known as the probability density function (PDF) can be used to analyze the shape of a distribution and its summary statistics. Comparing the histogram plots for both the raw and simulated proximate components, the similarities in both distributions can be observed. The upper and lower bounds of both distributions are very close, their upper and lower quartiles and median values are the same.

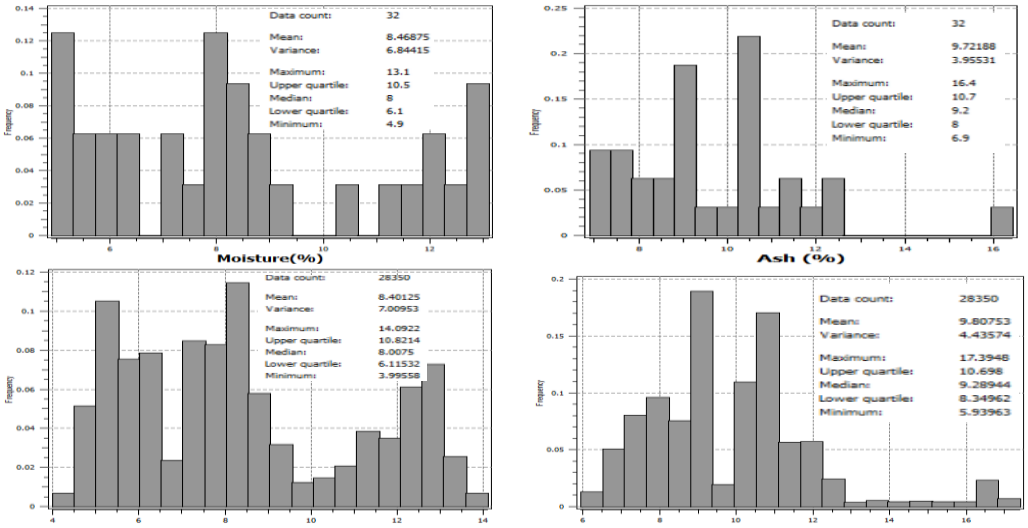

Compositional SGCS Moisture (%) Realization #99

Compositional SGCS Ash (%) Realization #99

Figure 26: Top-left Histogram plot of Raw-Moisture, Bottom-left Histogram plot of SGCS Moisture / Top-right Histogram plot of Raw-Ash, Bottom-right Histogram plot of SGCS Ash

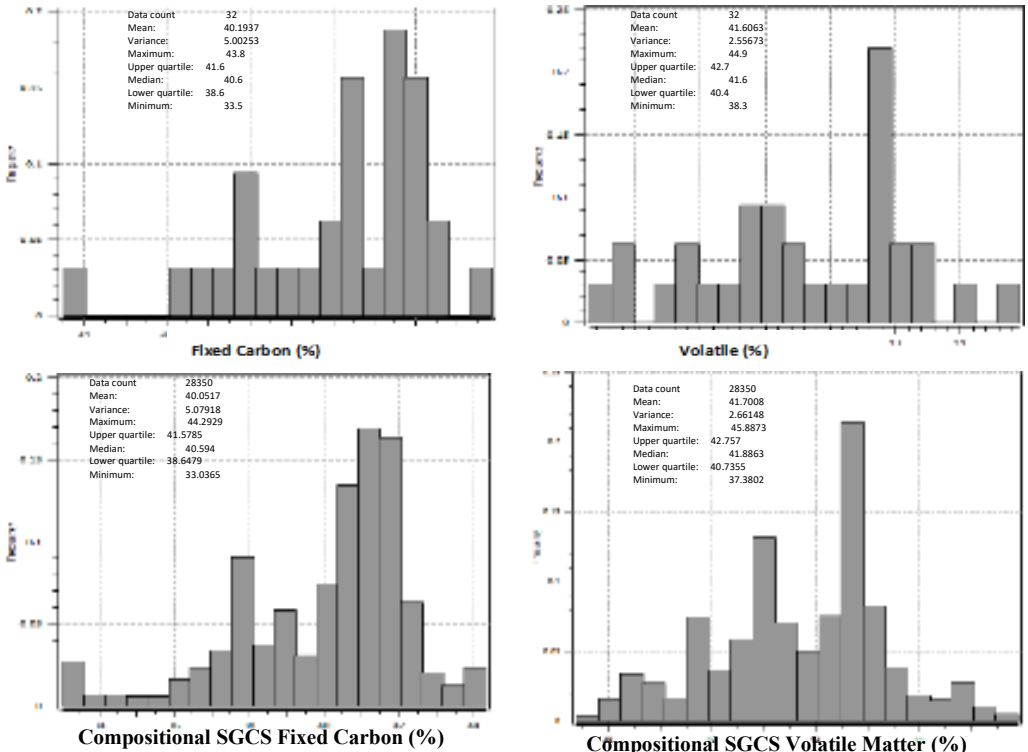

Compositional SGCS Fixed Carbon (%) Realization #99

Compositional SGCS Volatile Matter (%) Realization #99

Figure 27: Top-left Histogram plot of Raw-Fixed Carbon, Bottom-left Histogram plot of SGCS Fixed Carbon / Top-right Histogram plot of Raw-Volatile Matter, Bottom-right Histogram plot of SGCS Volatile Matter

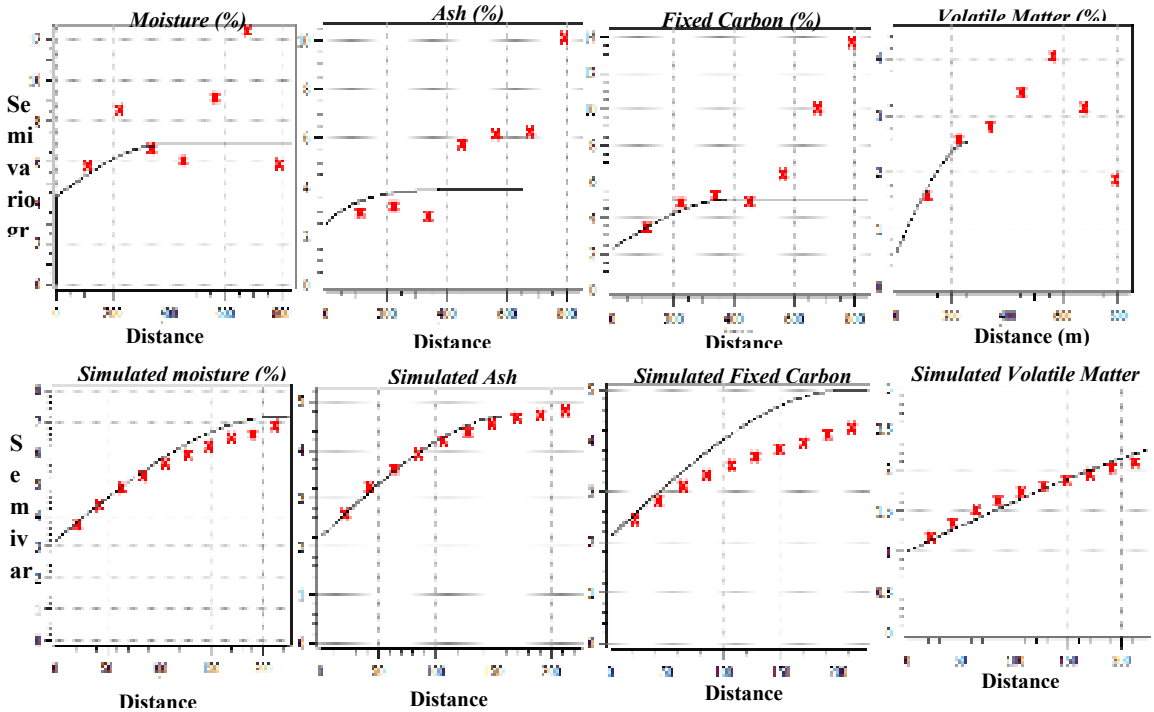

Figure 28: Top row shows the variograms of the raw proximate components, bottom row gives the variograms of the simulated proximate components.

The validating spatial continuity plots (variogram) in Figure 28, compares the spatial fluctuations of the simulated values and those of the original data. The variogram model parameters for the simulated values are given in Table 17, comparing them to the parameters in Table 16 (those of the raw proximate components), we can see the similarities, especially in the ranges, which mark the extent of spatial continuity of the values. Taking a closer look at the variogram model of the simulated components, we can observe that all the values plot on or below the variogram structure, none of the values went way above the sill until beyond the 350 m range mark (not captured in this plot for easy viewing purpose), this range is very close to those of the raw variogram structure. This implies that the spatial fluctuations of our simulated value and those of the original (raw) data are similar, which further confirms that our model, honours the data configuration, the histogram and variogram of the original data, and as such can be used for further analysis of the deposit- grade and tonnage computation of the coal deposit in the study area, which is the focus of the next section.

Table 17: Variogram Model Parameters for SGCS proximate analysis components

SGCS COMPONENT	MODEL	NUGGET	SILL- NUGGET (SILL CONTRIBUTION)	MIN. RANGE (A) (M)	MAX. RANGE(A) (M)
MOISTURE	spherical	3.2	3.95	200	350
ASH	spherical	2.2	2.53	200	350
FIXED CARBON	spherical	2.1	2.90	200	350
VOLATILE MATTER	spherical	1.0	1.66	200	350

Resource Estimation

BLOCK MODEL (Definition of Selective Mining Units (SMU))

In mining, the most important interest is in estimating a certain selective mining unit (SMU) that is a volume of material of a specific size that characterizes mining selectivity. [22], defined the SMU volume size as the minimum volume of material on which ore and waste can be separated, which is a function of mining method and selectivity. They also stated that the SMU size is related to the ability of the (excavator) equipment to select material; it is also based on the data available for ore/waste classification, the procedures used to

translate that data to minable dig limits, and the efficiency with which the mining equipment excavates those dig limits.

Considering the above factors together with the interpreted controls on mineralization, and geometry of mineralization, a SUM volume size of 10 x 10 x 1.7 m was chosen for the Onupi coal deposit block model. The block model (block/cell) was created and constrained by the validated geologic model (wireframe) for the coal seam (Figures 8 and 9). Figure 29 shows the constrained block model in the surpac window, with a vertical exaggeration of 5 for the Z-axis, the north direction is the same as that illustrated in Figures 8 and 9.

Table 18: Block model Report for the Onupi coal, generated using Surpac.

GEMCOM SOFTWARE INTERNATIONAL FEB 28, 2022				
BLOCK MODEL SUMMARY ONUPI_COAL_BLOCKMODL2.MDL				
ONUPI COAL BLOCK MODEL FOR RESOURCES ESTIMATION				
TYPE	**Y**	**X**	**Z**	
MINIMUM COORDINATES	823828	362500	260	
MAXIMUM COORDINATES	824778	362950	275.3	
USER BLOCK SIZE	10	10	1.7	
MIN. BLOCK SIZE	10	10	1.7	
ROTATION	0	0	0	
TOTAL BLOCKS	16124			
STORAGE EFFICIENCY %	70.09			
ATTRIBUTE NAME	**Type**	**Decimals**	**Background**	**Description**
ASH	Float	2	16.40	Ash-content (%)
CALORIFIC_VAL	Float	2	3018.96	Calorific value (Kcal/kg)
FIXED_CARBON	Float	2	43.80	Fixed carbon content (%)
MOISTURE	Float	2	13.10	Moisture content (%)
SEAM_THICKNESS	Float	2	1.70	Avg. seam thickness (m)
SG	Float	2	1.30	Specific gravity of sub-bituminous coal
THICKNESS	Float	2	2.25	coal seam thickness (m)
VOLATILE	Float	2	44.90	Volatile matter content (%)
BLOCK MODEL SUMMARY 1/1				

Table 18 gives the block model report, which contains the size for each cell, the total number of blocks (SMU), the attributes, viz, the proximate analysis components and their background (maximum) values, the average seam thickness and the specific gravity of subbituminous coal. These attributes are necessary as they will be used for the classification of the blocks into ore or waste, calculation of diluted grade, tonnage and recoverable product.

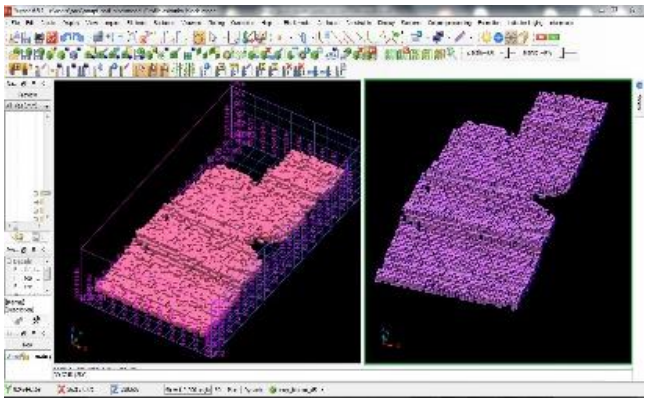

Figure 29: Left – the block model in a 50 x 50 x 10 grid without cell outline. Right – block model without grid and containing each cell outline. For proper viewing, a vertical exaggeration of 5 was applied to the Z-direction since it's smaller in length when compared to the X and Y – directions.

Block Model Population with simulated values

The SGSM function in the Gslib estimation option in surpac was used to populate the blocks, using the proximate analysis values and the exact spatial continuity parameters already discussed. One hundred realizations were ran. Realization # 99 was chosen and its values were assigned to the cells of the block model. Figure 30 shows the populated blocks for the fixed-carbon content.

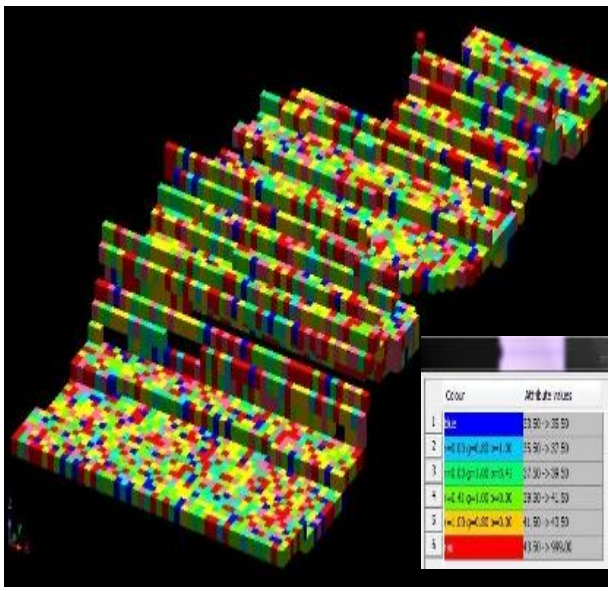

Figure 30: Block Model populated with simulated values for Fixed-Carbon (%) (Realization #99).

From the legend in Figure 30, the fixed-carbon content for each block (SMU) can be determined, blue coloured blocks indicate blocks with fixed-carbon content range of 33.50 – 35.50 % (low carbon content), and yellow and red coloured blocks with fixed-carbon content range of 41.50 % and above (high carbon content for subbituminous coal).

The quality of coal is generally determined by its fixed-carbon content and ash contents. In some cases, moisture content is also used as a coal quality determinate parameter. Based on the purpose for which the coal under study is used for, fixed-carbon (carbon) content value will be used as the coal quality (grade) determinate parameter. So, the grade of a block refers to the value of carbon contained in it. In the same vain, calorific value

of coal which is a measure of the heat energy released by coal is dependent on the carbon content, the higher the carbon content the higher the calorific value.

Block model Classification (Ore and Waste) - Cutoff Grade (CG) Definition

Proposing a generalized methodology for the computation of cutoff grade (grade that is normally used to discriminate/classify between ore and waste within a given deposit) is very difficult or impossible, as every mine has its unique features, and as such has its unique parameters used to define a cutoff grade. In this section a cutoff grade based on the fixed carbon content is defined for the Onupi coal to distinguish ore from waste.

The coal extraction operation in the study area is not for commercial purposes (the coal mined is not sold for profit) but used by the company to fire the kiln for cement production. Owing to this fact, the cutoff grade determinate parameters at Onupi are different from the traditional cutoff grade determinate parameters as profit from sale of coal is not the focus. At Onupi the CG is dependent on the ratio of the overburden thickness (OBT) to the coal seam thickness (CST) and Fixed-carbon content (FCC). Consequently, an average CST of 1.7 m, OBT less than 35 m and FCC of 33% and above were chosen as the cutoff grade defining parameters.

Dilution Factor

The National Instrument 43-101 (NI-43-101) requires that details about dilution (waste material that is not separated from the ore during the mining operation and is mined with ore) factor used for prefeasibility and feasibility reports for resource estimation be stated, but not necessarily for preliminary economic assessment (PEA) studies but can be assumed[41].It is generally accepted that dilution is about 5% for vain type deposits such as a copper porphyry, and about 10% for tabular (sedimentary) deposits such as a gold, coal etc.[42]. Owing to the non-disclosure agreement of some vital information between the company and the researchers most of the economic information in this work are informed assumptions, as such this section can be seen as a PEA studies. As a result, the dilution expression (Equation 18) was used to compute the dilution factor, and a dilution factor of 10% was applied to the resource and reserve estimation.

$$Dilution\ (\%) = \frac{waste\ tonnes}{(ore\ tonnes + waste\ tonnes)}\ x\ 100 \qquad (18)$$

Furthermore, from pit observation and drill core studies, the major sources of dilution at Onupi will come from the inter-burden between the upper and lower coal seams, and the shaly-coal layers that have a gradational contact with the main coal seams. This can be minimized by the skill of the excavator operator and the reduction of the bench height to allow for more selectivity during coal production.

Recoverable Resource Evaluation

The concept of recoverable resources imply that we are interested in evaluating a truncated statistic (a part) of the overall grade distribution. The classical formulae (Equations 19, 20 and 21) formulated by [43],and[22], for the evaluation of tonnage, metal quantity (in this case coal quantity) and average grade for recoverable material are found after defining an economic cutoff (threshold) for any set of SUM. The tonnage is simply the sum of all unit (block) tonnages that are above the threshold;

$$T_{(z_0)} = T_0[1 - F_z(z_0)] = T_o.\int_{Z_c}^{+\infty} fz(Z)dz = T_0\,.\,\frac{1}{N_A}\sum_{i=1}^{N_A} t_i(u_i, Z_c) \qquad (19)$$

Where T_0 is the total in-situ tonnage at a cutoff 0 and Z_c is the applied cutoff grade.

The quantity of carbon is calculated as the summation of the quantity of fixed-carbon for each individual unit;

$$Q_{(z_0)} = T_o.\int_{Z_c}^{+\infty} Z.\,fz(Z)dz = T_0\,.\,\frac{1}{N_A}\sum_{i=1}^{N_A} Z.\,t_i(u_i, Z_c) \qquad (20)$$

Where Z is the grade of the unit block.

Finally, the average grade of the recovered material (recoverable resource) is computed as the ratio of the contained material in tons to the total in-situ tonnage

$$M_{(z_0)} = \frac{Q_{(z_0)}}{T_{(z_0)}} \qquad (21)$$

The above parameters where applied to the block model to classify the blocks into ore and waste. Figures 31, 32, 33 and 34 shows the classified blocks in the surpac window and the attributes. During the classification, an ore-waste flag of 0 and 1(integer values) were used to discretize the blocks, the integer 0 signifies waste (blue blocks – blocks below the cutoff grade), and the integer 1 signifies ore (red blocks – blocks above the cutoff grade or threshold).

Figure 31 shows both ore and waste and the attributes for an ore block. Figure 32 shows only the waste blocks and the attributes of one block, and Figure 33 and Figure 34 shows only the ore blocks and the attributes for one block. In the attribute panel in the figures, the attributes for the block model in view are the ones with the suffix '_33'. The suffix '_33' is the identification used for fixed-carbon content greater-than 33%. Table 19 shows the attributes and their description.

Table 19: Attributes in blocks and their description

S/N	ATTRIBUTE	DESCRIPTION
1	Composite_grade_33	Composite grade calculated for that block, using a composite length of 1 m
2	Individual_ratio_33	The ratio of the volume of material (ore + waste) to that of the product (ore) for that block. A high value indicates that the block is not economical.
3	Cumulative_ratio_33	The ratio of volume of material to product for all blocks within a column.
4	Diluted_grade_33	The grade of the block after the dilution factor of 10% is applied.
5	Fixed_carbon	The raw fixed carbon content of the block before dilution factor is applied
6	Fixed_carbon 1	The simulated/estimated fixed carbon content of the block before dilution factor is applied.
7	Ore_waste_flag_33	The flag (integer value) that signifies if a block is ore or waste.
8	Recoverable_product_33	The part of the ore that can be recovered for that block, gotten after a recovery of 90% is applied.
9	Recovery_33	The recovery factor 90% (assumed), this means we have an ore loss (reduction) of 10%
10	Sg	Specific gravity of subbituminous coal.

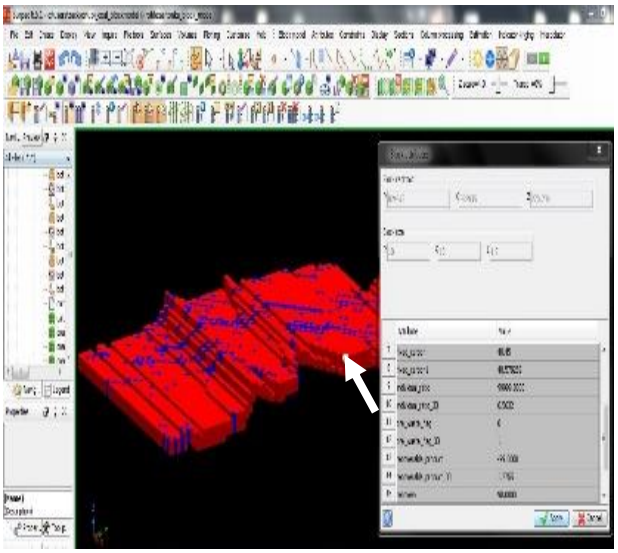

Figure 31: Block model classified into Ore (Red blocks) and Waste (Blue blocks) after the application of the cutoff grade parameters specific for Onupi Mine. The block attribute panel gives the attributes and the values for the block pointed by the arrow.

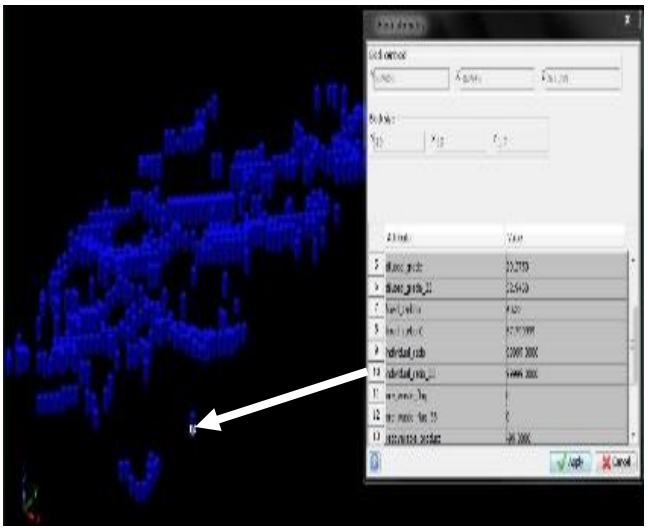

Figure 32: Blocks classified as waste (blocks that did not satisfy the grade cutoff constrains). The block attribute panel gives the attributes and the values for the block pointed by the arrow.

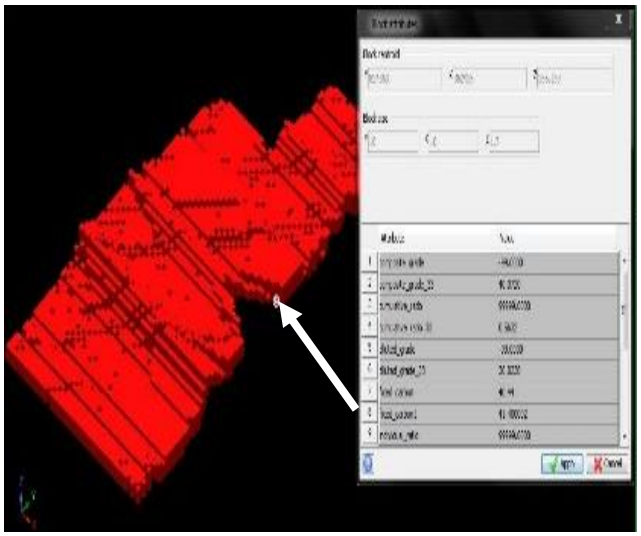

Figure 33: Blocks classified as Ore (blocks that satisfy the grade cutoff constrains). The block attribute panel gives the attributes and the values for the block pointed by the arrow.

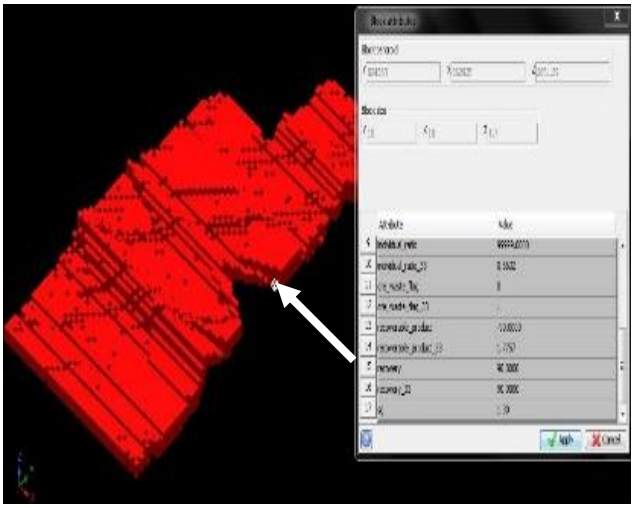

Figure 34: Blocks classified as Ore (blocks that satisfy the economic cutoff constrains).
The block attribute panel (continuation from Figure 33) gives the attributes and the values for the block pointed by the arrow.

GEMCOM SOFTWARE INTERNATIONAL
MAR 13 2022

BLOCK MODEL REPORT
BLOCK MODEL:
ONUPI_BLOCKMOD_33.MDL
VOLUME TONNAGE REPORT FOR ECONOMIC GRADE PARAMETERS AT ONUPI COAL: CST OF 1.7 M, OBT < 35 M, FIXED CARBON CONTENT > 33.0%.
CONSTRAINTS USED
A. NOT ABOVE DTM TOP_ORE_33.DTM OBJECT ID 1 TRISOLATION ID 1
B. ABOVE DTM BOT_ORE_20.DTM OBJECT ID 1 TRISOLATION ID 1
C. = BLOCK ORE_WASTE_FLAG 1

Z	Volume (m^3)	Tonnes (Mt)	Diluted Grade	Recoverable Product (m^3)
257.0 -> 259.0	58174.00	75626.00	27.88	84388.52
259.0 -> 261.0	182099.00	236728.00	26.65	252519.28
261.0 -> 263.0	243055.00	315971.00	26.68	337353.38
263.0 -> 265.0	363125.00	472062.00	27.30	515707.88
265.0 -> 267.0	416174.00	541026.00	27.36	592460.22
267.0 -> 269.0	437877.00	569239.00	27.23	620414.66
269.0 -> 271.0	305643.00	397336.00	27.28	433844.84
271.0 -> 273.0	99293.00	129080.00	26.68	137812.92
273.0 ->	36006.00	46808.00	26.51	49673.77

275.0				
275.0 -> 277.0	5826.00	7574.00	26.79	8121.33
GRAND TOTAL	**2147270.00**	**2791451.00**	**27.14**	**3032296.80**
			1/1	

Furthermore, the ore blocks were further classified into economic blocks (recoverable blocks) by applying an assumed recovery value of 90%. The cumulative volume of all economic blocks was calculated and the specific gravity applied to convert from volume to tonnage. Table 20 gives the result of the volume, tonnes, diluted and recoverable product for the economic blocks, calculated at 2-meter interval along the Z-axis (downwards).

Table 20: Volume, Tonnage and Recoverable Product Report for the economic blocks at the study area generated.

From Table 20, a total volume of 2,147,270 cubic meter of coal, with a weight of 2,791,451 metric tonnes, having a fixed carbon content greater-than 33%, and an aggregate recoverable product of 3,032,296.80 cubic meter of coal was estimated within the study area in Onupi.

Tonnage- Cutoff Grade Curve

Tonnage-cutoff grade curves are common tools in reserve evaluations, used to analyze the relationship between tonnages at different cutoff grades, which allows to predict recoverable resources in an SMU at different economic cutoff grades. Figure 35 gives the Tonnage – cutoff grade chart for some selected grade cutoff based on fixed carbon content. Table 21 gives the tonnage and grade cutoff values.

From Figure 35, the inverse relationship between carbon cutoff and carbon tonnage can be observed. It means at higher cutoffs low carbon tonnages should be expected. So, if we place or assign high carbon cutoffs for the coal deposit or SMU, the quantity (tonnage) of coal that would be available for production will be low, as such economic cutoff grade assignment will differ for different SMU's within the Onupi coal field.

Table 21: Selected Grade cutoff and their evaluated tonnages

GRADE CUTOFF	TONNAGES
47	1739075
46	2898600
45	1936000
36	1012440
33	3161836
28	7562600
27	4949150
26	1472320

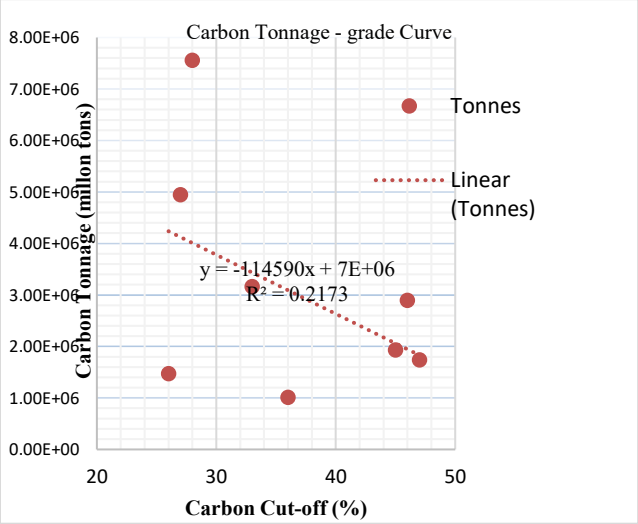

Figure 35: Tonnage-Cutoff Grade Curve Based on Fixed Carbon Content (%)

Resources and Reserves Classification

Mineral Resources

According to the Canadian Institute of Mining, Metallurgy and Petroleum (CIM) guidelines in NI 43-101 standards of disclosure for mineral projects**,** the public disclosure of estimated resources requires that resource estimates be classified based on degree of confidence and allocated as measured, indicated and inferred, while reserves must be classified as either proven or probable reserves, derived under certain rules from resources categories [22].

Measured Mineral Resources: Mineralization or other natural material of economic interest may be defined as a measured mineral resource when the nature, quality, quantity and distribution of data are such that the tonnage (quantity) and grade (quality) of the mineralization can be estimated to within close limits and that the variation from the estimate would not significantly affect potential economic viability.

Indicated Mineral Resources: Mineralization may be classified as an indicated Mineral Resource when the nature, quantity and distribution of data are such as to allow confident interpretation of the geological framework and to reasonably assume the continuity of mineralization. The importance of the Indicated Mineral category to the advancement of the feasibility of the project and as a base for major development decisions must be recognized by the Qualified Person (QP).

Inferred Mineral Resource: Mineralization can be classified as Inferred Mineral Resource if the quantity and grade (quality) can be reasonably assumed, but not necessarily verified. As a result of the uncertainty that maybe attached to Inferred Mineral Resources, it cannot be assumed that all or any part of an Inferred Mineral Resource will be upgraded to an Indicated or Measured Mineral Resource as a result of continued exploration. Confidence in the estimate is not sufficient to permit meaningful application of technical and economic parameters or to enable an economic evaluation viable enough for public disclosure. As such, Inferred Mineral Resources must be excluded from estimates forming the basis of feasibility or other economic studies [22].

Mineral Reserves

A Mineral Reserve is the economically minable (extractable) part of a Measured or Indicated Mineral Resource displayed by a least a Preliminary Feasibility Study. This study must contain sufficient information on mining, processing, metallurgical, economic and other relevant factors that demonstrate, at the time of reporting, that economic extraction can be justified or validated. A mineral Reserve includes diluting materials and allowances for losses that may occur when the material is extracted. A mineral Reserve can be classified as Proven or Probable Mineral Reserve.

A Proven Mineral Reserve is the economically mineable part of a Measured Mineral Resources demonstrated by at least a Preliminary Feasibility Study which must include, adequate information on mining, processing, metallurgical, economic, and other relevant factors that demonstrate, at the time of reporting, that economic extraction is justified. On the other hand, a Probable Mineral Reserve is the economically minable

part of an indicated, and in some circumstances a Measured Mineral Resource displayed by at least a Preliminary Feasibility Study,[22].

Resource and Reserve Classification for the Onupi Coal

From the above definitions of Resource and Reserve, and the consideration of the geological and economic factors specific for the Onupi coal. The classification of the coal in the study area into Resource is given in Tables 22 and 23.

Table 22: Measured and Indicated Resources

MEASURED/INDICATED RESOURCES				
Z	Volume	Tonnes	Diluted Grade	Recoverable Product
259.0 -> 261.0	182099.00	236728.00	26.65	252519.28
261.0 -> 263.0	243055.00	315971.00	26.68	337353.38
263.0 -> 265.0	363125.00	472062.00	27.30	515707.88
265.0 -> 267.0	416174.00	541026.00	27.36	592460.22
267.0 -> 269.0	437877.00	569239.00	27.23	620414.66
269.0 -> 271.0	305643.00	397336.00	27.28	433844.84
271.0 -> 273.0	99293.00	129080.00	26.68	137812.92
273.0 -> 275.0	36006.00	46808.00	26.51	49673.77
GRAND TOTAL	2083272.00	2708250.00	26.96	2939786.95

Table 23: Inferred Resource

INFERRED RESOURCES				
Z	Volume	Tonnes	Diluted Grade	Recoverable Product
257.0 -> 259.0	58174.00	75626.00	27.88	84388.52
275.0 -> 277.0	5826.00	7574.00	26.79	8121.33
GRAND TOTAL	64000.00	83200.00	27.34	92509.85

The Measured and Indicated Resources in Table 22 can pass as proven Mineral Reserve for the study area after proper evaluation of relevant mining, processing and economic factors, whose details are not within the scope of this work. From Table 22, the total Measured and Indicated Resources is 2,708,250.00 tonnes at a recoverable product of 2,939,786.95 tonnes, and from Table 23, the total Inferred Resource is 83,200.00 tonnes, and Recoverable product of 92,509.85 tonnes.

CONCLUSION

The creation of a geologic model from drill cores analysis that intersected the coal seam, and from studies of excavated sections within the ore domain, together with the production of coal quality maps by applying both the ilr transformation and sequential simulation, allows for the integration of both geologic and statistical models of the deposit, thus providing a resource estimation result with high confidence. The integration of geologic and statistical models provides in depth knowledge of the spatial extent of the coal

deposit and also the distribution of the attributes across the deposit, which are very useful information during mine planning.

More so, by applying ilr transformation and sequential simulation for data modeling, several maps (realizations) that allows clear characterization of the coal quality across the deposit were produced, from which the best map that depicts the original raw data characteristics was chosen.

The semivariograms used for modeling were free of any spurious correlations that would have been present if ilr transformation was not used. Semivariogram studies showed significant spatial correlation among the ilr balances, which led to the choice of cosimulation for resource estimation.

Normality test revealed that the balances were not approximately normal, thus warranting the transformation of the data into normal space to properly apply sequential gaussian simulation. Additionally, model validity analysis showed that the histogram and semivariogram of the chosen realization was the same as those of the parent (raw) data.

The Tonnage-Cutoff grade curve shows a general inverse relationship between Tonnage and Cutoff grade for the Onupi coal. From where we drew inference that, at higher carbon grade cutoffs,coals with low carbon contents should be expected. As such economic cutoff grade assignment will differ for different SMU's within the Onupi coal field.

Resource estimation and classification carried out on the geologic block model with SUM dimensions (volume) of 10 x 10 x 1.7 m^3 showed that the estimated resource of the coal deposit in Onupi field was estimated to have a total volume of 2,147,270 cm^3 with a tonnage of 2,791,451 MT and a fixed carbon content (grade) greater than 33%. The total measured and indicted coal resource (reserve) in the study area is approximately 2,708,250.00 MT, while the inferred resource is 83,200.00 MT.

Funding:
"This research received no external funding"

Data Availability Statement:
Data used in this research – the proximate analysis result and the drill core field report were obtained from the Dangote Coal Mine Onupi (a privately-owned company) and is not publicly archived.

Acknowledgments:
We are grateful to the Dangote Coal Mines especially the geology, survey and mining teams for allowing us work with them, and also granting us access to their data used in this work.

Conflicts of Interest:
The authors declare no conflict of interest.

REFERENCE

[1] Schopf, J.M. (1956). *A Definition of Coal*. *Society of Economic Geologist, Inc., 51,* pp 521-527
[2] Stopes, M.C. & Wheeler, R. V. (1918). Monograph on the constitution of coal: Department of Science and Industry Research, London, pp 1-58.
[3] Stutzer, O. & Noe, A. C. (1940). *Geology of coal*: University Chicago Press, pp 461.
[4] Arkell, W. J. & Tomkeieff, S. I. (1953).*English rock terms*. London: Oxford University Press, pp 140.
[5] Rosemary, F. (2013). *LECTURE NOTE on coal geology, types, ranks and grades.*www.fossilfuel.co.za> Rosemary PDF coal geology, types, ranks and grades- Fossil Fuel Foundation.
[6] World Coal Institute. (2005).*The Coal Resource; A Comprehensive Overview of Coal*. https://www.worldcoal.org>file_val...The Coal Resource- A Comprehensive Overview of…World Coal Association.
[7] American Association for Testing of Material (ASTM), (2013). *Standard practice for proximate analysis of coal and coke*. ASTM Standard D3172-13 (pp.2).
[8] Bacon-Shone, J., 2011. A short story of compositional data analysis. In: Pawlowsky-Glahn, V., Buccianti, A. (Eds.), Compositional Data Analysis: Theory and Applications. John Wiley and Sons Ltd., Chichester, UK, pp. 1–11.
[9] Caers, J. (2011): *Modeling Uncertainty in the Earth Sciences*. Wiley-Blackwell; Chichester, 2011, UK: p. 229.
[10] Chile`s, J.P., Delfiner, P., (2011). *Geostatistics: Modeling Spatial Uncertainty*, *2nd edn. Wiley Series in Probability and Statistics*, New York, p. 695.

[11] Molayemat, H., Torab, F.M., Pawlowsky-Glahn, V., Morshedy, A.H., Egozcue, J.J., (2018). *The Impact of the compositional nature of data on coal reserve evaluation, a case study in Parvadah IV Coal deposit, Central Iran.* Inter. Jorl. of Coal Geology. https://doi-org/10.1016/j.coal.2018.02.003.

[12] Olea, R.A., Karacan, O.C., (2018): *Mapping of Compositional properties of Coal using Isometric log-ratio transformation and Sequential Gaussian Simulation- A comparative study for spatial ultimate analysis data*. J. Geochem Explor.2018 March, 186: 24-35. doi:10.1016/j.gexplo.2017.11.022.

[13] Olea, R.A., Luppens, J.A., (2015). *Mapping of coal quality using stochastic simulation and isometric logratio transformation with an application to a Texas lignite*. Int. J. Coal Geol. 152 (PA), 80–93. Available at: http://www.sciencedirect.com/science/article/pii/S0022169414006386.

[14] De Swardt, A.M.J., Casey, O.P., and Jefford, G. (1963): *The Coal Resources of Nigeria. Bulletin No.28,* Published by the Ministry of Mines and Power, Geological Survey of Nigeria.

[15] Fatoye, F.B. & Gideon, Y. B. (2013). Appraisal of the Economic Geology of Nigerian Coal Resources. *Journal of Environment and Earth Science, 3* (11), pp 35-46.

[16] Obaje, N. G. & Hamza, H. (2000). Liquid Hydrocarbon Source-rock Potential of Mid-Cretaceous Coals and Coal Measures in the Middle Benue Trough of Nigeria. *International Journal Earth Sciences, 89* (130), pp 139.

[17] Carter, J. D., Barber, W., Tait, E. A. & Jones, G. P. (1963). The Geology of Parts of Adamawa, Bauchi and Borno Provinces in North-eastern Nigeria. *Bulletin Geological Survey Nigeria, 30*, pp 1 – 108.

[18] Obaje, N. G., Ligouis, B. & Abba, S. I. (1994). *Petrographic Composition and Depositional Environments of Cretaceous Coals and Coal Measures in the Middle Benue Trough of Nigeria.* International Journal Coal Geology, 26, pp 233 – 260.

[19] Ojoh, K. A. (1992). *The Southern part of the Benue Trough (Nigeria) Cretaceous Stratigraphy, Basin Analysis, Paleo-oceanography and Geodynamic Evolution in the Equatorial Domain of the South Atlantic*. NAPE Bull 7, p.131–152.

[20] Umeji, A.C., (2000). *Evolution of the Abakaliki and the Anambra Sedimentary basins, Southeastern Nigeria*. Project Rpt. to SPDC Ltd, p. 155.

[21] Nwajide C.S., (2013). *Geology of Nigeria's Sedimentary Basins - Anambra Basin,* p. 304-336. Published by CSS Bookshops Limited Lagos. www.cssbookshopslimited.com

[22] Rossi, M.E., Deutsch, C.V., (2014): *Mineral Resource Estimation*. www.springer.com, https://doi-org/10.1007/978-1-4020-5717-5.8. p. 337.

[23] Pawlowsky-Glahn, V., Egozcue, J.J., Tolosana-Delgado, R., (2015a). *Modeling and analysis of compositional data*. In: Statistics in Practice. John Wiley & Sons, Cichester, UK (272 pp).

[24] Pawlowsky-Glahn, V., Egozcue, J.J., Lovell, D., (2015b). *Tools for compositional data with a total. Stat. Model.* 15 (2), 175–190. Available at: http://www.scopus.com/inward/record.url?eid=2s2.084926148988&partnerID=40&md5=7384168d65cc077624e60a5215cc6f8a.

[25] Reimann, C., Filzmoser, P., Garrett, R.G., Dutter, R., (2008). *Statistical data analysis explained*. In: Statistics, pp. 359. http://dx.doi.org/10.1002/9780470987605.

[26] Pawlowsky-Glahn, V., Egozcue, J.J., (2006). *Compositional data and their analysis: an introduction*. Geol. Soc. Lond., Spec. Publ. 264 (1), 1–10. http://dx.doi.org/10.1144/GSL.SP.2006.264.01.01.

[27] Pawlowsky-Glahn, V., (1984). *On Spurious Spatial Covariance between variables of Constant Sum*. *Science de la Terre*, 21, 107-113.

[28] Egozcue, J.J., Pawlowsky-Glahn, V., Mateu-Figueras, G., Barceló-Vidal, C., (2003). *Isometric Logratio transformations for compositional data analysis*. Math. Geol. 35(3), 279–300.

[29] Comas, M., Thió-Henestrosa, S., (2011). *CoDaPack 2.0: a stand-alone, multiplatform compositional software.* In: Egozcue, J.J., Tolosana-Delgado, R., Ortego, M.I. (Eds.), Proceedings of the 4th International Workshop on Compositional Data Analysis, Sant Feliude Guixols. International Center for Numerical Methods in Engineering ((10 pp.) http://ima.udg.edu/codapack/).

[30] Aitchison J. (1983) *Principal component analysis of compositional data.* Biometrika. 1983, 70(1):57–65.

[31] Otero N, Tolosana-Delgado, Soler A, Pawlowsky-Glahn V, Canals A., (2005) *Relative vs. Absolute statistical analysis of compositions: a comparative study of surface waters of a Mediterranean river.* Water Res. 2005; 39(7):1404–1414. [PubMed: 15862341]

[32] Deustch, C.V., Journel, A.G., (1997): *GSLIB- Geostatistical Software Library and User's Guide*, 2nd edn. Oxford University Press, New York. p. 369.

[33] Olea, R.A., Pawlowsky-Glahn, V., (2009). *Kolmogorov–Smirnov test for spatially correlated data*. Stoch. Env. Res. Risk A. 23 (6), 749–757.www.springer.com, https://doi-org/10.1007/s00477-008-0255-1

[34] Pyrcz, M.J., Deutsch, C.V., (2014). *Geostatistical Reservoir Modeling*: New York, Oxford University Press, second edition, (433 pp.).

[35] Mohamad, N.H., (2013): *Introduction to Geostatistics for Resources Evaluation and Estimation* (unpublished lecture notes). Jurusan Teknik Pertambangan Fakultas Teknik, Universitas Negeri Padang, Padang. 1 April, 2013.www.scribd.com/document/17378019/Introduction-to-Geostatistics-UNP-pdf.

[36] Remy, N., Boucher, A., Wu, J., (2009). *Applied Geostatistics with SGeMS—A User's Guide*. Cambridge University Press, Cambridge, UK (264 pp.).

[37] Srivastava, R.M., (2013). *Geostatistics: a toolkit for data analysis, spatial prediction and risk management in the coal industry*. Int. J. Coal Geol. 112, 2–13.

[38] Goovaerts, P., (1997): *Geostatistics for Natural Resources Evaluation*. Oxford University Press, New York, p. 483.
[39] Abzalov, M.Z., (2016): *Applied Mining Geology*. www.springer.com/series/7377. p. 443
[40] Verly, G. (1993): *Sequential Gaussian Cosimulation: A simulation method integrating several types of information*. In: Soares A (ed) Geostatstics Troia`92. Vol 1. Wuwer Academic Publishers, Dordrecht, p. 543-554.
[41] Canadian Securities Administrators (2012), *National Instrument 43-101 Standards of Disclosure for Mineral Projects (NI 43 – 101)*.https://www.securities-administrators.ca
[42] Anoush, E., (2013). *An attempt to standardize the Estimation of dilution factor for Open pit mining Projects. (The importance of Dilution Factor for Open pit Mining Projects)*. World Mining Congress, Montreal 2013. www.srk.com
[43] Journel, A.G., Huijbregts, C.J., (1978): *Mining Geostatistics*. Academic Press, New York.